The Effect of Electric and Magnetic Fields Near an HVDC Converter Terminal on Implanted Cardiac Pacemakers

EPRI

EPRI EA-1511
Project 679-1-3
Final Report
August 1980

Keywords:
HVDC Converters
Magnetic Fields
Cardiac Pacemakers
Electric Fields

Prepared by
IIT Research Institute
Chicago, Illinois

ELECTRIC POWER RESEARCH INSTITUTE

The Effect of Electric and Magnetic Fields Near an HVDC Converter Terminal on Implanted Cardiac Pacemakers

EA-1511
Research Project 679-1-3

Final Report, August 1980

Prepared by

IIT RESEARCH INSTITUTE
10 West 35th Street
Chicago, Illinois 60616

Principal Investigator
M. J. Frazier

Prepared for

Electric Power Research Institute
3412 Hillview Avenue
Palo Alto, California 94304

EPRI Project Managers
H. A. Kornberg
L. Sagan

Health Effects and Biomedical Studies Program
Energy Analysis and Environment Division

ORDERING INFORMATION

Requests for copies of this report should be directed to Research Reports Center (RRC), Box 50490, Palo Alto, CA 94303, (415) 965-4081. There is no charge for reports requested by EPRI member utilities and affiliates, contributing nonmembers, U.S. utility associations, U.S. government agencies (federal, state, and local), media, and foreign organizations with which EPRI has an information exchange agreement. On request, RRC will send a catalog of EPRI reports.

NOTICE

This report was prepared by the organization(s) named below as an account of work sponsored by the Electric Power Research Institute, Inc. (EPRI). Neither EPRI, members of EPRI, the organization(s) named below, nor any person acting on their behalf: (a) makes any warranty or representation, express or implied, with respect to the accuracy, completeness, or usefulness of the information contained in this report, or that the use of any information, apparatus, method, or process disclosed in this report may not infringe privately owned rights; or (b) assumes any liabilities with respect to the use of, or for damages resulting from the use of, any information, apparatus, method, or process disclosed in this report.

Prepared by
IIT Research Institute
Chicago, Illinois

ABSTRACT

The electromagnetic fields associated with HVDC converters and transmission lines constitute a unique environment for persons with implanted cardiac pacemakers. A measurement program has been conducted to assess the potential interfering effects of these harmonically rich fields on implanted pacemakers. The experimental procedures that were employed take into account the combined effects of the electric and magnetic fields. The effect of the resulting body current on the response of six pacemakers was assessed in the laboratory, using a previously developed model to relate body current to pacemaker pickup voltage. The results show that R-wave pacemaker reversion can be expected at some locations within the converter facility, but that a large safety margin for unperturbed pacemaker operation exists beneath the transmission lines.

Blank Page

EPRI PERSPECTIVE

PROJECT DESCRIPTION

This report describes the second of two studies conducted by IITRI to investigate the interaction of high-voltage (HV) electromagnetic (EM) environments with implanted cardiac pacemakers. The first (RP679-1), entitled The Effects of 60-Hertz Electric and Magnetic Fields on Implanted Cardiac Pacemakers, examined interactions beneath 60-Hz HV overhead lines.

This report (RP679-1-3) attempts to clarify the hazard potential of the EM environment around DC converters. This environment is considerably more complex than that which exists beneath overhead lines because in converting AC to DC (or vice versa) the converter terminal generates fields with many frequency components.

PROJECT OBJECTIVES

The study was designed to subject pacemakers on the laboratory bench to the same EM interference they would receive were they implanted in persons located in or near an HVDC converter facility. The research team first went to Bonneville Power Administration's Celilo converter terminal and recorded the electric and magnetic signals on tape. Seven different sites in and around the converter were chosen for recording, in order to represent all the possible signal mixes found in the converter vicinity. In the laboratory the signals were played back into the pacemakers, and pacemaker sensitivity to interference was recorded. The sensitivity is reflected in the magnitude of interference signal it takes for a pacemaker to enter reversion, a mode in which the device pulses the heart asynchronously.

PROJECT RESULTS

The data show that absolutely no interference is to be anticipated under DC transmission lines once outside of the converter facility. The study also showed (as did the earlier study by IITRI) that reversion is also improbable on the AC side outside of the facility. Reversion is probable, however, at various locations

within the confines of the converter terminal. Susceptibility to reversion varied among the devices tested. It should be emphasized that the consensus of cardiologists is that reversion is not considered hazardous to pacemaker wearers.

The following points should also be noted when reading the report:

1. Celilo as a test terminal may give the wrong impression about the exposure risks in HVDC terminals. Present terminal designs in the U.S. are much more compact. Given that the newer designs will possibly reduce field exposures, the effects from the valve commutations seen at sites 4 and 5 will be less likely.

2. The study considered a complex electromagnetic environment and did not attempt to discriminate between E-field and B-field induced reversion, nor did it attempt to plot pacemaker sensitivity as a function of frequency. An earlier report (EPRI EA-1174) by the same group discusses E-field and B-field sensitivity at 60 Hz in depth.

EPRI will extend its pacemaker program with an evaluation of exposed human pacemaker patients (University of Rochester, RP679-6). All subjects will be under constant medical supervision. We believe that at its conclusion the program will have comprehensively addressed the issue of HV electromagnetic interference with implanted cardiac pacemakers.

Robert Kavet, Project Manager
Energy Analysis and Environment Division

ACKNOWLEDGMENTS

The author wishes to thank Dr. A. R. Valentino, Manager of the IITRI EM Effects Section, for guidance and assistance; Mr. R. A. Zalewski for the design of the electric and magnetic field sensors, and Mr. S. Tumarkin for assistance with the laboratory and field experimental work. Appreciation is extended to Ms. L. Wyatt for typing the manuscript.

The author also wishes to thank Mr. P. Eichen of BPA for his assistance and coordination in the field testing effort and the staff of the Celilo HVDC terminal for their cooperation and assistance.

Respectfully submitted,

IIT RESEARCH INSTITUTE

M. J. Frazier
Senior Engineer

APPROVED

A. R. Valentino, Manager
EM Effects Section

Blank Page

CONTENTS

Blank Page

ILLUSTRATIONS

Blank Page

TABLES

Section 1

SUMMARY

Electric and magnetic fields in the ELF frequency range cause current to flow in the body of a person who is in the field. If the person wears an implanted electromedical device, such as a cardiac pacemaker, potentials at the frequency of the ELF field will be induced on the electrodes and leads of the implanted medical device. The potentials (voltages) so induced on the medical device represent an interference signal which, in some instances, may adversely affect the performance of the device.

Past work on the present EPRI contract resulted in an assessment of the effects of the electric fields from 60 Hz EHV transmission lines on implanted pacemakers. The task being reported here was to investigate the effects that fields associated with HVDC conversion might have on implanted pacemakers.

The conversion of HVAC to HVDC results in the production of significant harmonic components of the 60 Hz primary frequency. The waveform of harmonically rich signals is highly dependent on both the amplitude and phase of the various harmonic components. Past investigations have shown that the response of pacemakers to interfering signals is a function of the waveshape of the interference. Thus, concern was expressed that the harmonically-rich electric and magnetic fields associated with HVDC converter terminals might provide a more severe interference than the low-harmonic fields from 60 Hz EHV lines.

The assessment of pacemaker response to HVDC converter electromagnetic fields was accomplished in two steps. First, measurements were made at seven representative locations within the Bonneville Power Administration (BPA) Celilo HVDC

converter station. The principal data collected at each measurement location consisted of magnetic tape recordings of real time signals proportional to the time derivative of both the electric and magnetic fields.

As a second step, the recorded waveforms were played back, appropriately scaled in amplitude and impressed across the input of six pacemakers in the laboratory. All but one of the pacemakers were of the R-wave inhibited type; the other was an R-wave synchronous type. The amplitude of the signal impressed across the pacemakers in the laboratory bench test was related to the signal amplitude that would be developed across a pacemaker implanted in a person standing at the field measurement site. The scaling procedures assumed a worst-case implant configuration for the pacemaker.

The investigations which have been performed on this task have shown that

1. When operating asynchronously, none of the pacemakers tested were affected in any way by the recorded waveforms, even when the waveforms were amplified to many times what would be expected at the pacemaker terminals.

2. When operating with a simulated R-wave, all of the pacemakers responded (reversion to the asynchronous mode*) when subjected to the waveform recorded at Site #1 and #5. Two pacemakers responded to the interference which could be expected at Site #3. With varying degrees of safety margin, none of the waveforms recorded at the other sites would be expected to cause interference.

The program results suggest that risk to pacemaker wearers within these facilities is quite minimal, since only reversion to the asynchronous mode was observed. However, since only a limited number of pacemakers was tested, assurance cannot be given that other less desirable responses might not occur for some pacemakers at these field levels.

---

*Brief reversion of a cardiac pacemaker to the asynchronous mode, with or without competition from the patient's intrinsic cardiac rhythm, is not considered of significant risk for patients sufficiently ambulatory to walk in these locations.

The program results also suggest that if the measured fields below the HVAC and HVDC lines outside the converter station are representative, then there is little or no chance of any perturbation of implanted pacemaker operation as a result of these fields.

Section 2

INTRODUCTION

The influence of fields associated with a HVDC converter station on implanted pacemakers has been investigated. This work is an extension of the investigation into the effects of 60 Hz EHV electric fields on implanted pacemakers. The results of the 60 Hz investigation have been previously reported (1).

The electromagnetic fields associated with HVDC converter stations are harmonically rich, due to the nonlinear conversion process. The voltage that is induced into implanted pacemakers by these fields has the harmonic components further accentuated as a result of the pickup transfer function, which increases in amplitude linearly with frequency.

The use of harmonically-rich laboratory-generated signals to test pacemaker susceptibility to simulations of the HVDC environment is not a credible approach. Pacemaker susceptibility has been noted to be dependent on interference signal waveshapes; and the waveshape of harmonically rich signals is highly dependent on the amplitude and phase of the harmonic components. Therefore, it follows that pacemaker testing must be performed with signals derived from the actual fields, for harmonically rich or complex waveform fields.

To facilitate realistic pacemaker testing, signals related to the fields were recorded in real time. These real-time waveforms were then used to test pacemaker susceptibility.

The voltage developed across an implanted pacemaker is not related to the electric or magnetic fields by a constant. The voltage is proportional to the time derivative of the fields; thus the higher frequency components are emphasized. Rather than record real time signals proportional to HVDC converter fields, the approach used on this program was to use electric and magmetic field sensors whose output was proportional to the time derivative of the field. Thus, the recorded signal due to either the electric or magnetic field

was related by a constant to that component of voltage which would be developed across an implanted pacemaker.

Prior to this task, IITRI had developed the analytical procedures to relate the interference voltage across implanted pacemakers to either an electric or magnetic field in the ELF frequency range. These procedures were used on this task to determine the constant which related the field sensor outputs to the voltage that would be developed across an implanted pacemaker. Since the voltage developed across a pacemaker is dependent on the lead arrangement used for the implant, near worst-case lead arrangements were assumed, i.e., an arrangement resulting in near maximum voltage pickup.

The sensors and real time recording procedures were used to measure the electric and magnetic fields at seven representative locations associated with the world's largest HVDC converter terminal. This facility is the Celilo converter in Oregon, which is operated by the Bonneville Power Administration.

The signals so recorded were used to test a total of six representative production line pacemakers from three leading manufacturers. Five of the pacemakers were of the R-wave inhibited type while the sixth was R-wave synchronous.

The tests were performed by previously used "bench test" procedures. The pacemakers were tested with and without a simulated ECG signal in addition to the interference.

The following section, Section 3, presents a brief review of the salient aspects of modern-day pacemakers and implant procedures which are relevant to ELF interference considerations. Section 4 presents a review of the manner in which both low frequency electric and magnetic fields develop interfering potentials across the input circuitry of implanted pacemakers. Section 5 describes the procedures and instrumentation used on this program for measuring and recording the real time signals of importance for implanted pacemakers, due to the electric and magnetic fields associated with HVDC converter facilities. Section 6 describes the BPA Celilo HVDC converter facility; the sites where

measurements were made on this program; and presents examples of the data collected at these sites. Section 7 describes the manner in which the signals which were recorded at the measurement sites were used to test representative pacemakers in the laboratory. Also presented in Section 7 are the results of the pacemaker testing effort.

Section 3

CARDIAC PACEMAKERS--A REVIEW

All cardiac pacemakers function by stimulating the heart by means of electrical impulse applied directly to the ventricle. The pulses which are emitted from the pacemaker are at a nominal rate of 70 beats per minute, although higher or lower pulsing rates can be obtained from the manufacturer or can be programmed into some pacemakers. At least four types of pacemakers can be identified, the types differing in their sensing and pacing functions in relation to the cardiac electrical output waveform or ECG waveform. Figure 3.1 shows a typical external ECG waveform which can be used to illustrate the timing involved in the operation of various types of pacemakers which are asynchronous, P-wave synchronous, R-wave synchronous, and R-wave inhibited. The R-wave inhibited pacemaker is by far the most common pacemaker employed at this time. It is commonly quoted that between 90 to 95 percent of all current implants are of the R-wave inhibited type. Thus, the study of the R-wave inhibited pacemaker is most appropriate.

The R-wave inhibited pacemaker senses the R-wave portion of the ventricular electrical activity, designated by the letter R in Figure 3.1. This type of pacemaker emits a stimulating pulse whenever the absence of a detected signal exceeds a pre-determined time interval. Whenever an R-wave is present, the pacemaker output is inhibited so that the pacemaker is completely inactive during periods of normal heart activity.

The reason for this design feature is that the majority of pacemaker patients have rate and rhythm disturbances which are intermittent; hence, they depend on artificial pacemaker stimulation only when the intrinsic heart rate falls below a preset minimum level. Accordingly, the majority of pacemaker patients now receive such non-competitive pulse generators that will artificially pace the heart only when needed, and which will not compete with the patient's own characteristic cardiac rhythm.

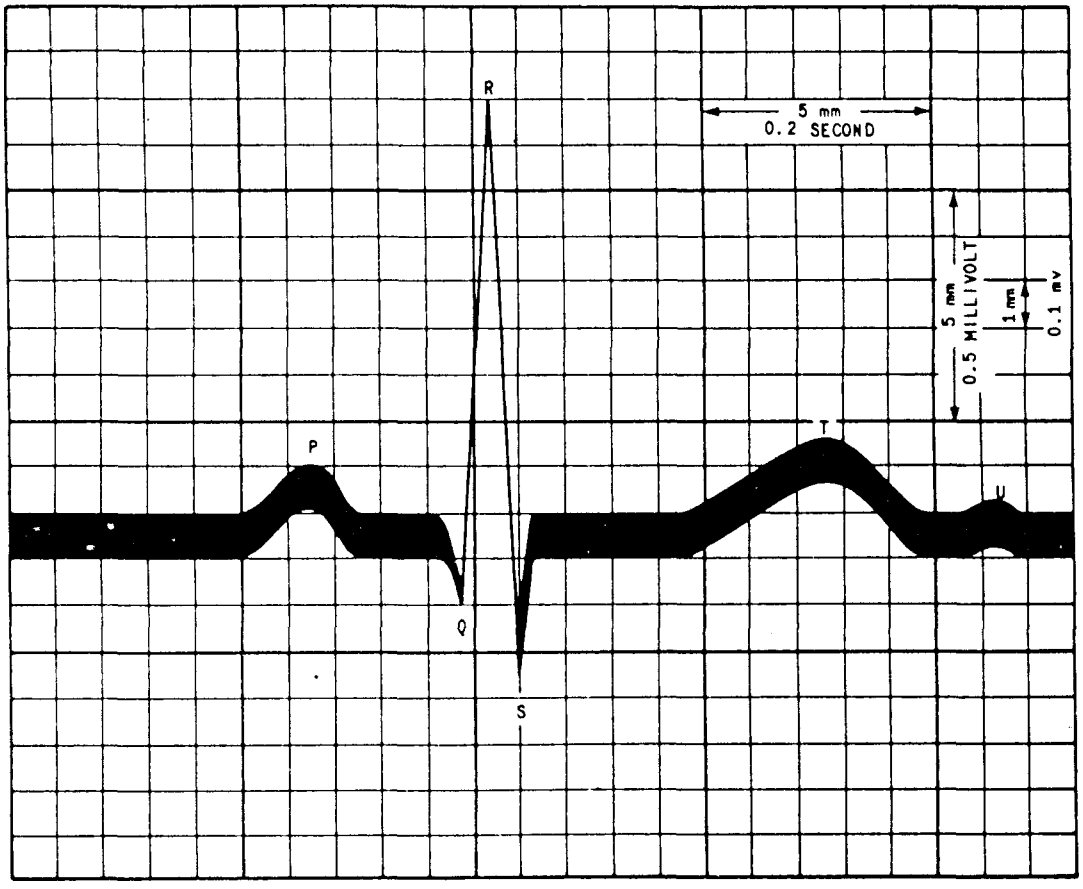

Figure 3.1 NORMAL ECG WAVEFORM

In addition, the R-wave inhibited pacemaker incorporates sensing logic to detect the presence of interference which might falsely inhibit the pacemaker. When interference is sensed, the pacemaker reverts to the asynchronous mode. In the asynchronous mode, the pacemaker produces pulses at a preset rate.

A pacemaker is also classified with regard to the types of leads employed. Both monopolar and bipolar leads are used, with some pacemakers being convertible from one type to the other. In the monopolar configuration, a single lead carries the stimulating impulse from the pulse generator to the heart. The return path is via body tissue back to the pulse generator which provides a metallic contact with the body tissue and serves as a second electrode.

In the bipolar configuration, two conductors run from the pulse generator to the heart. The two conductors may be physically separated and insulated, or they may run together in a common insulating jacket. In general, bipolar endocardial leads are configured in a common jacket; and the electrodes, which are separated by 15-30 mm, make contact with the endocardium. For bipolar myocardial pacing, two individual insulated leads, which may actually be monopolar leads, are frequently used. The electrodes of the two leads are placed approximately 2.5 cm apart on the ventricular epicardium.

From the standpoint of ELF potentials developed at the pacemaker input due to electric fields or body currents, the significant difference between monopolar and bipolar pacemakers is the distance separation between electrodes. The potential developed across two electrodes, situated in a resistive material through which current is flowing, is proportional to the electrode spacing. Therefore, because of the greater separation, it may be expected that monopolar implants will encounter larger ELF potentials than will bipolar implants.

A variety of implantation techniques are used. When a monopolar lead is used, the implant site of the pulse generator becomes important, since the pulse generator metal case usually serves as the second electrode. The pacemaker electronics package or pulse generator is usually located in either the

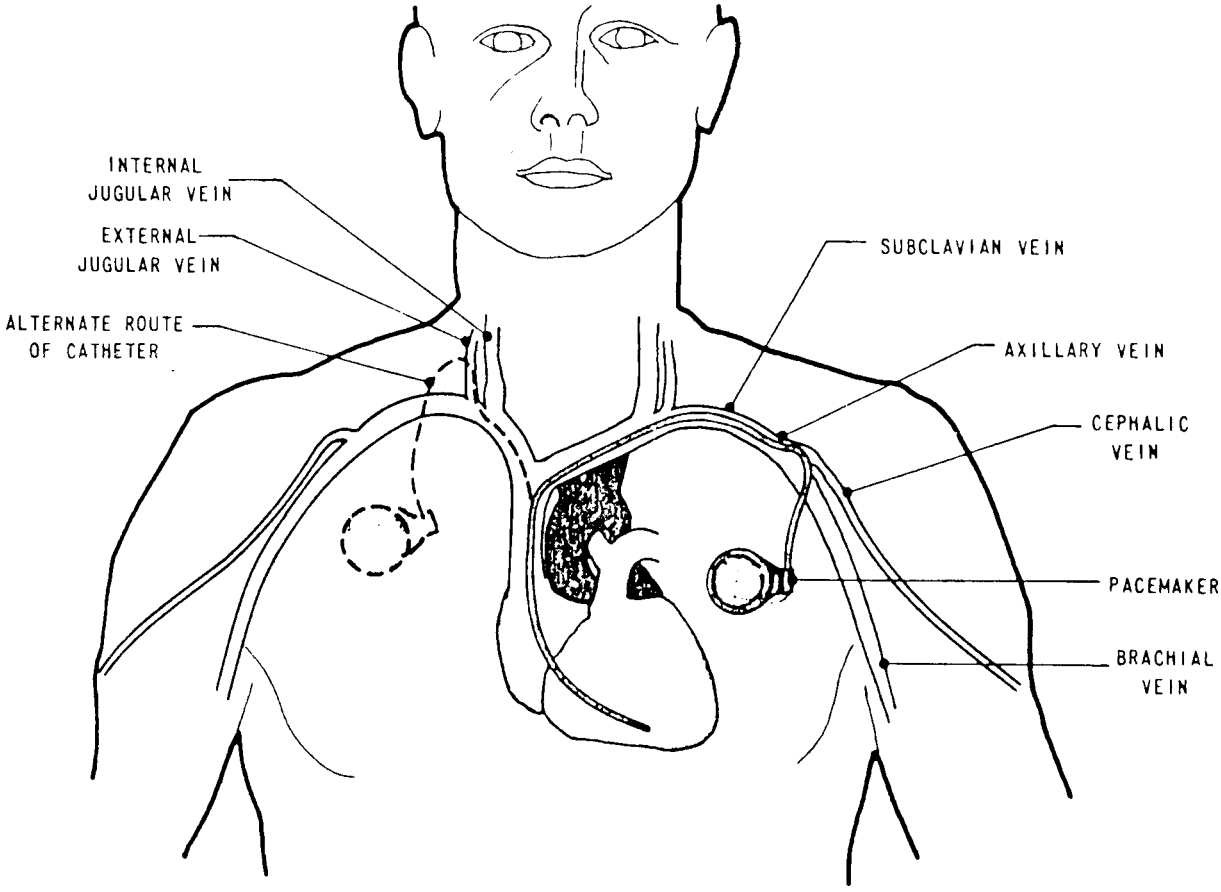

Figure 3.2 HUMAN ENDOCARDIAL IMPLANTATION

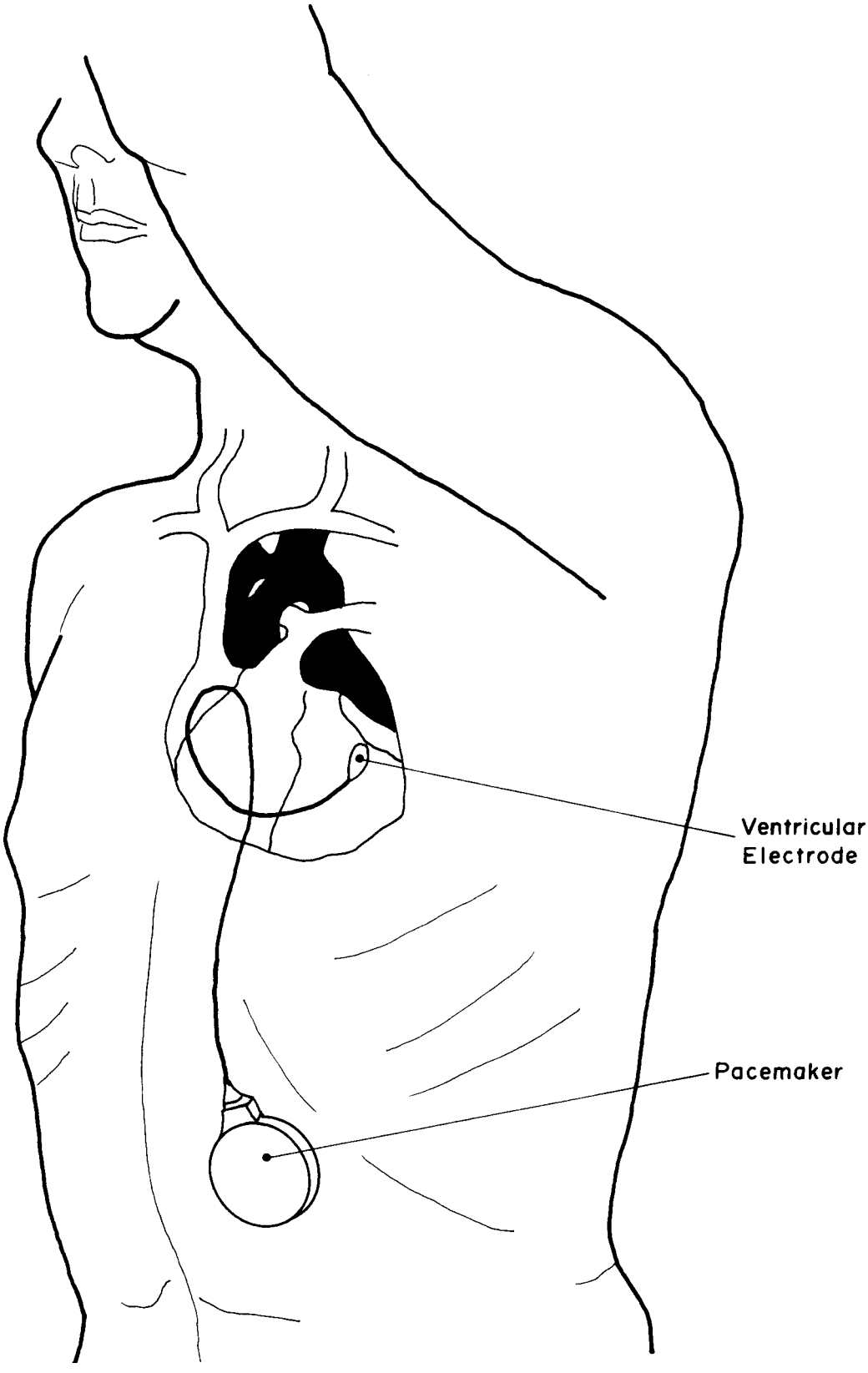

Figure 3.3 HUMAN EPICARDIAL IMPLANTATION

abdominal or pectoral region, as shown in Figures 3.2 and 3.3. It is seen that the pulse generator configuration shown in Figure 3.3 has a maximum separation between the heart electrode and the position of the pacemaker. If a monopolar configuration is used, that is, where one of the electrodes is the pulse generator and the remaining electrode is on or within the heart, a very significant separation between the two electrodes exists. This configuration gives rise to maximum ELF voltage being induced between the pacemaker electrodes for a person standing erect in a vertical electric field while grounded through the feet. In the monopolar case, where the pulse generator is implanted in the right or left pectoral region, body currents induced from vertical electric fields generally result in smaller induced voltages than for the abdominal implant site.

For constant amplitude sinusoidal interfering signals, such as 60 Hz, the only effect on pacemaker operation to be anticipated is reversion to the asynchronous rate. Typically, the transition to the asynchronous mode occurs at some level of interfering 60 Hz potential at the pacemaker input terminals. For high harmonic content waveforms, such as anticipated in and around HVDC converter terminals, the pacemaker response was unknown prior to the efforts of this program. However, prior investigations had shown that the pacemaker response to non-sinusoidal interference is highly dependent on the interference waveshape.

The reversion of the pacemaker to the asynchronous mode during periods where interference is present and when the heart is functioning normally, generally results in competition between the spontaneous electrical activities of the normally functioning heart and the electrical stimulus applied by the pacemaker. Agreement appears to exist that brief transitory reversion to this asynchronous mode is acceptable. For example, physicians test implanted pulse generators by applying an external magnet over the unit which de-activates the sensing circuits. The 15-60 seconds of artificially induced competition produced by this technique has not caused any clinical problems for these situations for ambulatory patients. In the case of longer periods of competition, there seems to be no agreement among cardiovascular specialists about the seriousness (or sometimes, even the existence) of problems associated with prolonged competition due to interference induced reversion to the asynchronous mode.

Section 4

REVIEW OF ELF FIELD INDUCED PICKUP IN IMPLANTED PACEMAKERS

GENERAL CONCEPTS

The procedures for relating ELF electric or magnetic fields to the potential which appears across the input of an implanted cardiac pacemaker have been developed by IITRI. The susceptibility of cardiac pacemakers to ELF magnetic fields was studied by IITRI on a program for the U.S. Naval Electronic Systems Command, Washington, D.C. (2). The primary objective of this program was to determine a safe level (threshold) for magnetic fields in the 60 Hz frequency range. Under this program, a procedure for in vitro testing of pacemakers was developed, and several representative pacemakers were characterized. To test the actual in vivo magnetic field pickup, several implants were made in calves. The measured pickup was assessed by determining the effective loop area by both x-ray procedures and autopsy. The test results and procedures were extended to the human form by studying the x-rays of humans with implanted pacemakers. The study showed that loop areas fall in the range of 45 to 210 cm^2. The methods and procedures developed under the above program have been thoroughly documented by Miller, et al (2).

In an earlier portion of this contract for the Electric Power Research Institute, IITRI developed procedures and modeling techniques to permit the evaluation of the effects of ELF electric fields on implanted cardiac pacemakers. This study used pacemakers implanted in non-human primates to obtain a basic understanding of how the electric fields affect the implanted pacemakers. The animal tests provided a good understanding of the relative sensitivity of various types of implants to electric fields or conducted body current flow. A semi-empirical model was developed to provide a quantitative estimate of the relationship between the external electric field and the potential developed across pacemakers implanted in adult humans. The model was validated by in vivo testing of implanted pacemakers in the non-human primates. The details of this study are comprehensively documented by Bridges and Frazier in a prior report under this contract (1).

In the next few paragraphs, the salient aspects of the above two efforts will be reviewed to provide the reader with an understanding of how the electric and magnetic fields couple to an implanted pacemaker. At the frequencies of concern, any interference to implanted pacemakers which may occur, is a result of a potential being developed across the input terminals of the pacemaker circuitry. The potential which is developed at the pacemaker input is a result of the pacemaker leads and implanted electrodes. That is, interfering signals are not directly induced into the pacemaker circuitry by the fields for well-designed modern pacemakers.

For the case of electric field excitation, it has been shown that the pacemaker pickup is directly related to the separation between the implanted body contacting electrodes. Furthermore, for the case of a person standing in a vertical electric field, the voltage developed across the pacemaker is a function of the vertical distance between the implanted pacemaker electrodes, and is not a function of the electrode location on any plane that is normal to the body axis. This condition occurs due to the fact that all points in the body that lie on a plane normal to the body axis, for a person standing in a vertical electric field, are equipotential. Thus, for electrodes located within the body at heights h_1 and h_2 above the ground, the potential developed between these electrodes is independent of their position so long as h_1 and h_2 remain constant.

For electric field excitation, the body in its most basic form, is considered as a chain of resistors, as shown in Figure 4.1. The electric field causes a current to flow through the body which is not a constant, but varies as a function of position along the body, as is depicted in Figure 4.1. Due to this non-uniform current, different voltages will be developed across the various resistors in the chain, as illustrated in the figure. Since the input impedance of a pacemaker is high relative to tissue impedance, the pacemaker will sense the voltage developed across the intervening tissues between its electrodes, due to the current flowing through that tissue. Thus, again referring to Figure 4.1, if the position of the pacemaker electrodes is known with respect to the position along the resistor chain, the voltage developed across the implanted electrodes is readily determined, once the value of the resistors and the current as a function of position are known.

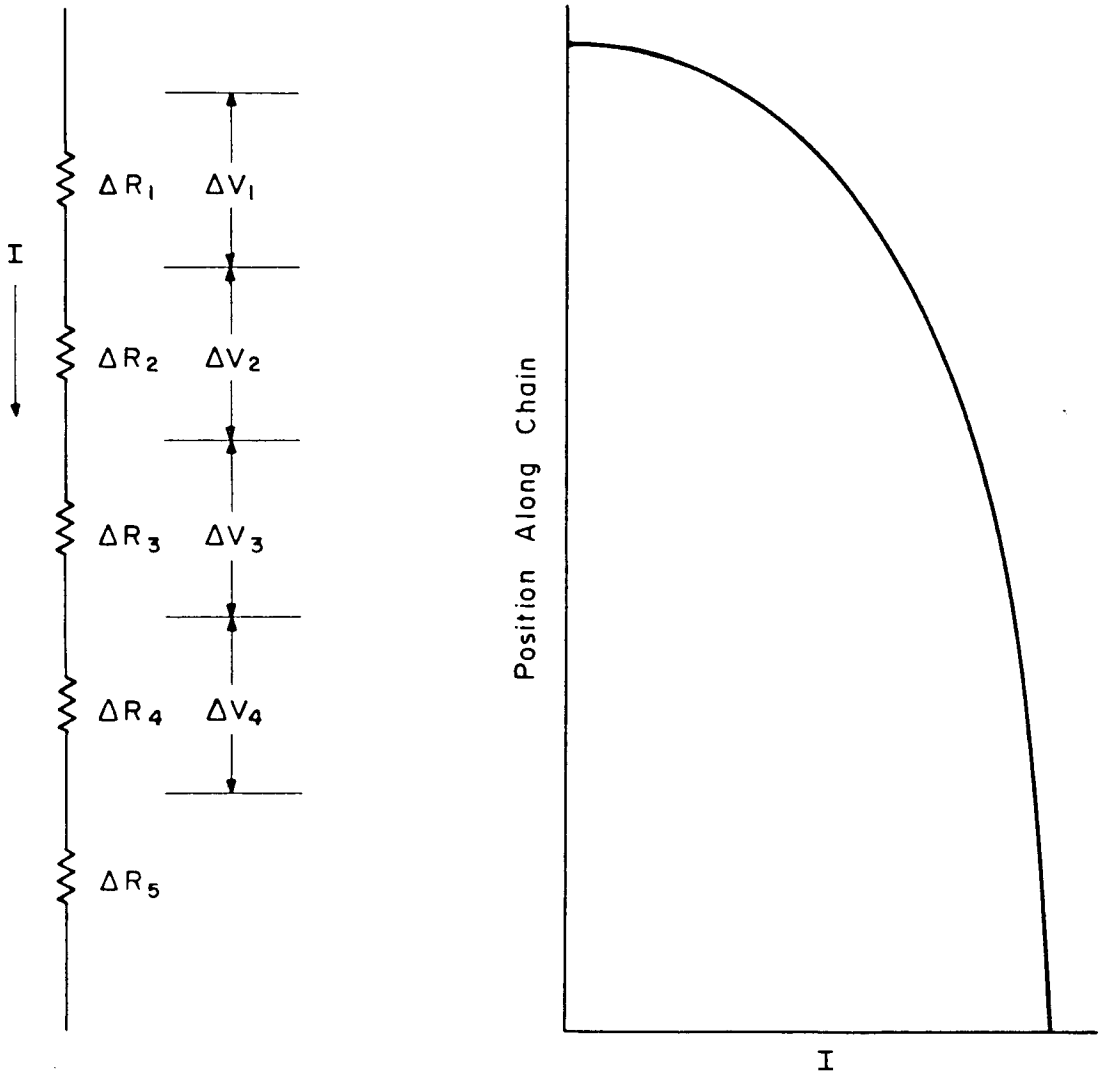

Figure 4.1 RESISTOR CHAIN REPRESENTATION

From the above considerations, it becomes evident that the voltage that will be sensed by an implanted pacemaker due to ELF electric fields is dependent on the type of implant, which often controls the separation between electrodes, and is a function of the pacemaker type, i.e., whether the pacemaker is a monopolar or bipolar unit. The electrode separations for bipolar pacemakers are, in general, considerably less than for monopolar units. For monopolar-type pacemakers, implants in which the pulse generator is located in the abdominal region typically will sense more voltage due to ELF fields than will, for example, a pectoral implant, since the vertical separation between the pectoral region and the heart catheter is, in general, somewhat less than the vertical separation between the abdominal region and the heart catheter. However, the important parameter is electrode separation; thus, if a pectoral implant has a larger vertical electrode separation than an abdominal implant, the pectoral implant may be subject to larger interference voltages.

In contrast to electric fields, low-frequency magnetic fields readily penetrate the body. A conducting loop will have a potential developed due to magnetic flux density which is normal to the effective plane of the loop. The leads of an implanted pacemaker form an effective loop within the body, and thus can have a voltage induced by a magnetic field. For monopolar leads, conduction is through the lead to the heart, and back through the body tissue to the pulse generator which comprises the second electrode. The effective loop includes the metallic electrode lead and the tissue path from the heart back to the pulse generator. For bipolar pacemakers, which have both leads in common sheath, the effective loop area is, in effect, negligible.

The following paragraphs provide additional information on the voltage induced across implanted pacemakers due to the electric and magnetic fields in the ELF frequency range.

THE COLLECTION OF BODY CURRENT DUE TO ELECTRIC FIELDS

When a conducting object is placed in a time-varying electric field, the field will cause a current to flow on the object. Since a person is a conducting object, currents will be induced onto a person when the person is in an electric

field. Of particular interest is the case where a person stands erect in a vertical electric field. The induction process can be viewed as an interception of displacement currents, by an area related to the geometry of the body. The induction can also be viewed from the standpoint of short antenna theory. In either case, predictions can be made to assess the currents which will flow to ground through the body when contact is made with the earth.

When a person is not grounded to earth, the fields will still cause current to flow in the body. However, the magnitude of this current will be less than when the person is grounded, or highly coupled to the ground via the capacitance between his feet and the ground.

Prediction of the field-induced body current can be made strictly on a theoretical basis. However, a significant body of empirical data exists on the amount of body current which flows to ground due to electric field induction for persons standing in an electric field. Extensive measurements made on both human subjects and metallized mannekins, as reported by T.D. Bracken (1976) (3) and D.W. Deno 1977) (4), agree quite well and show that the current flow to ground from a human subject in an electric field can be approximated by the relation

$$I_{sc} = 5.4 \times 10^{-9} h^2 E \quad . \tag{4-1}$$

This expression relates the current flow from the person to ground in amperes to the person's height, h in meters, and the electric field intensity, E, in volts per meter. If the body is viewed as an area collector of displacement currents, the short circuit current to ground from the person is given by

$$I_{sc} = \omega \varepsilon E A_h \quad . \tag{4-2}$$

In this expression, ω is the radian frequency of the field, ε is the free space dielectric constant, E is the field intensity in volts per meter, and A is the effective area of the conducting object, in this case, a person. Deno (1977) (4), provides an expression for the effective area of a grounded erect human as

$$A_h = \pi(h \tan 35.7^o)^2 \qquad (4\text{-}3)$$

Thus, the effective area of a person is directly proportional to the person's height squared. If the dimensions of a 50-percentile man are used, as given by H. Dreyfuss (1959) (5)

$$h = 1.755 \text{ meters} \quad .$$

From Eq. 4-3 and this height, it is found that the effective area is very close to 5 square meters. Thus, an ideal displacement current sensor, having an area of 5 square meters, would collect the same amount of current-to-ground as a typical human standing erect in the field while being well grounded to the earth plane.

The above considerations relate to the amount of current that flows from a person to ground when the person is in an electric field. However, the current which flows in the person is not a constant as a function of position along the height of the person. Bridges and Frazier (1976) (1) have utilized measurements in a saline-filled cylinder to determine an approximate relationship for the total current as a function of the vertical position in a tall, slim object. They showed that the current flow can be quite closely approximated by Eq. 4-4, over the lower 90% of the cylinder.

$$\begin{aligned} I_{s(z)} &= I_{sc}\left[1\text{-}0.69\ \left(\frac{z}{h}\right)^{2.14}\right] \\ &= \omega\varepsilon E A_h\left[1\text{-}0.69\ \left(\frac{z}{h}\right)^{2.14}\right] \end{aligned} \qquad (4\text{-}4)$$

In this expression, $I_s(z)$ is the total body current which flows through a cross-section at a height z; I_{sc} is the short circuit current-to-ground from the feet; and h is the total height of the cylinder or person. This expression was shown to compare quite favorably over the lower 70% portion of the height, with the current distribution data obtained with a metallized mannekin by Deno (1977) (4).

The expression given in Eq. 4-4 provides a reasonably simple relationship for the current distribution on the body, for vertical electric field excitation. It is felt to be quite valid over the regions of the body which are of concern, that is, in the region of the thorax, where the pacemaker and associated leads will be implanted.

PACEMAKER VOLTAGE DUE TO ELECTRIC FIELD INDUCED BODY CURRENT

As shown in Figure 4.1, the current flow induced into the body by the electric field causes potentials to be developed across the equivalent body resistances in the chain. Bridges and Frazier (1976) have shown by measurements made on volunteer test subjects, that the equivalent linear resistance along the thorax, expressed in ohms/cm, is relatively constant along the thorax. The expression used to determine the potential between two implanted electrodes, located at heights z_a and z_b, respectively, above the ground plane, is given by the expression

$$V_{ab} = \int_{z_b}^{z_a} RI(z)dz. \tag{4-5}$$

In this expression, R is the linear resistance of the thorax in ohms/cm; V_{ab} is the voltage resulting across the implanted electrodes; and I(z) is the current flow as a function of the vertical position z along the body axis.

For electric field excitation, the current flow as a function of position along the body was given in Eq. 4-4. Substituting this expression into Eq. 4.5 and performing the integration, for R being independent of position, gives potential across the implanted electrodes as

$$V_{ab} = \omega\varepsilon E A_h R\left[(z_a - z_b) - \frac{0.22}{h^{2.14}}\left(z_a^{3.14} - z_b^{3.14}\right)\right] \tag{4-6}$$

In this expression, the location of the implanted pacemaker electrodes, z_a and z_b, must be known in order to determine the voltage which will appear across the implanted pacemaker electrodes.

In section 3, use was made of the 50-percentile man to define typical locations for implanted pacemakers and electrodes. For monopolar-type pacemakers, where the pulse generator serves as one electrode, reference to Figure 3.1 indicates that the separation between electrodes for a typical abdominal monopolar implant is somewhat larger than for a monopolar pectoral implant. Some cardiologists have suggested that the electrode separations for some pectoral implants may be larger than for abdominally implaced pulse generators. However, since no definitive data are known to exist, the dimensions identified in Figure 3-1 for an abdominal implant will be used for the work which follows. This condition will be reasonably representative for pacemaker electrode separations of approximately 15 cm.

Thus, for assessing the effects of measured fields from a HVDC terminal on pacemakers, by means of bench test procedures, the dimensional values for use in Eq. 4-6 are:

Z_a = 122 cm

Z_b = 107.5 cm

h = 175.5 cm.

Based on the dimensions of the 50-percentile man, and extensive data on thorax resistivity obtained by R. Gamboa (6), Bridges and Frazier (1976) (1) have used a value of linear resistance of 0.79 ohms/cm as the value for R in Eq. 4-6. Substituting these quantities as well as the effective area and the free space dielectric constant, ε, into Eq. 4-6 results in Eq. 4-7, which is the expected voltage which will appear across the pacemaker for a typical abdominal monopolar implant as a function of the electric field and its frequency.

$$V_{ab} = 2.3 \times 10^{-9} fE \qquad (4\text{-}7)$$

In Eq. 4-7, f is the frequency of the field in Hertz, E is the electric field in volts/meter, and V_{ab} is the voltage at the pacemaker input in volts. Thus, it is seen that as the frequency of the field increases, the field required to produce a given voltage across the pacemaker decreases proportionately.

PACEMAKER VOLTAGE DUE TO MAGNETIC FIELD

D.A. Miller (1971) (2), determined from the examination of human pacemaker implant x-rays, that the effective loop areas for magnetic field pickup ranged from 45 to 210 cm^2. The voltage induced in the loop formed by the pacemaker lead and effective return path through the body to the pacemaker, appears directly across the pacemaker input circuitry. The voltages created by the magnetic field induction and the electric field induction, are phasors and add in this sense at the input to the pacemaker. The magnitude of the magnetic field induced voltage into a single turn loop is given by the expression

$$V'_{ab} = 2\pi fBA \times 10^{-8} \quad . \tag{4-8}$$

In this expression, a prime has been used on the received voltage to differentiate it from that induced across the pacemaker input by the electric field. In this expression, the area is expressed in square centimeters, the frequency is in Hertz, and the magnetic field density, B, is expressed in gauss. Using the worst-case area of 210 cm^2 as determined by D.A. Miller (1971), the voltage across the pacemaker is given by

$$V'_{ab} = 1.32 \times 10^{-5} fB \tag{4-9}$$

where, again, the frequency is in Hertz and the magnetic field flux density is in gauss. It is seen that this expression, similar to that shown in Eq. 4-7 for the electric field, is directly proportional to the frequency of the applied field.

Section 5

FIELD MEASUREMENT INSTRUMENTATION AND PROCEDURES

Both the electric and magnetic fields can induce a voltage across the input of an implanted cardiac pacemaker. The voltage induced by the electric field is proportional to the vertical separation between the pacemaker electrodes, and the voltage induced by the magnetic field is proportional to the effective loop area of the pacemaker lead and the return path back through the body to the pacemaker, for a monopolar implant. When both electric and magnetic field components are simultaneously present, the total voltage developed across the pacemaker input is the phasor sum of the individual voltages induced by the two fields. The voltage induced by either the electric or magnetic field component is directly proportional to the frequency of the field. Thus, in order to assess the effect of HVDC converter fields on implanted cardiac pacemakers, the measurement instrumentation should meet the following requirements.

- Signals related to the fields should be recorded in real time. These real time recordings could thus be later used for the purpose of bench testing pacemaker response.
- The recorded signals should be directly proportional to the voltage which would be sensed by implanted pacemakers. That is, the sensed voltage due to each field component should be proportional to the frequency of the incident field.
- The signal related to each field component should be separately recorded, to facilitate appropriate scaling and calibration for use in the bench testing of the pacemakers.
- The phase relationship between the two components of voltage should be maintained to permit the proper phase addition of the signals for testing the pacemaker response to the combined signal.

The measurement instrumentation and procedures were chosen to meet the above requirements.

DISPLACEMENT CURRENT SENSOR

In Section 4 it was shown that the current flow to ground from a person is proportional to the magnitude of the electric field, its frequency, and the

effective area of the person. It was also shown (see Eq. 4-7), that the voltage which appears across the pacemaker input, due to the electric field, is proportional to these same factors. A sensor which responds to the product of the electric field magnitude and its frequency is called a displacement current sensor. Such a sensor responds to the time derivative of the displacement density D, or equivalently, to the time derivative of the electric field intensity E. This type of sensor is referred to, in shorthand notation, as a $\dot{D}$ or $\dot{E}$ sensor, where the dot above the vector quantity denotes the time derivative.

The electrodes of a displacement current sensor are, in general, flat plates, which may be either rectangular or circular. Typically, a displacement current sensor is made such that one electrode is at ground potential. A second flat plate is placed a small distance above the ground plate and insulated from it, thus, in effect, forming a parallel plate capacitor. The charge induced on the top plate is related to the displacement density, D, and the area, A, of the plate by the expression

$$Q = D \cdot A = \varepsilon E \cdot A \qquad (5\text{-}1)$$

Since the displacement density is related to the electric field intensity by the free space permittivity, ε, the charge is also related to the electric field intensity, as shown in Eq. 5-1. If a connection is made between the plates, the charge will be transferred between the top plate and the ground reference electrode at the frequency of the time-varying field. Since the current is the time derivative of the electric field

$$I = \varepsilon \dot{E} \cdot A = j\omega\varepsilon E \cdot A \quad . \qquad (5\text{-}2)$$

If the plates are connected together by a resistor, R, the voltage developed across this resistor will be proportional to the electric field and its frequency,

$$V_p = j2\pi f\varepsilon E \cdot AR \quad . \qquad (5\text{-}3)$$

The sensor fabricated for use on this program is shown in Figure 5.1. The surface area of the plates was nominally 0.5 m^2, while the nominal plate separation was 4.75 cm. In order for the area expressed in Eq. 5-3 to be the physical area of the plates, it is necessary to use a guard ring surrounding the top plate, to minimize fringing field effects. For convenience, and to maintain a reasonable physical size of the sensor for shipment and use in the field, a guard ring was not employed for the sensor fabricated on this program. However, in order to relate the output voltage, V_p, of the sensor to the electric field magnitude, it was necessary to know the effective area of the plate sensor.

The effective area of the plate sensor was determined by calibrating the sensor in the IITRI field simulation facility. This facility is described in Bridges and Frazier (1976) and was used for animal testing of in vivo pacemaker performance for electric field excitation. For calibration, the sensor was placed in the facility and the ground plate connected to the ground electrode of the facility. A 60 Hz electric field was established in the facility and measured using the IITRI spherical electric field probe. The output voltage from the sensor was measured using several values of resistance. The effective area of the sensor determined in this manner was 0.858 m^2. The value of resistance used between the plates for the field tests was 10,000 ohms. This value of resistance and the measured effective area of the plates, when substituted into Eq. 5-3, results in Eq. 5-4 which relates the voltage out of the sensor to the magnitude of the electric field and its frequency. In Eq. 5-4, the frequency is in Hertz, and the electric field, E, is in volts/meter, while the probe output voltage, V_p, is in volts.

$$V_p = 4.77 \times 10^{-7} fE \qquad (5\text{-}4)$$

The above expression for the displacement current sensor can be compared to Eq. 4-7 for the voltage developed across the input to an abdominally located monopolar pacemaker. It is seen that

$$\frac{V_p}{V_{ab}} = 2.07 \times 10^2 \quad . \qquad (5\text{-}5)$$

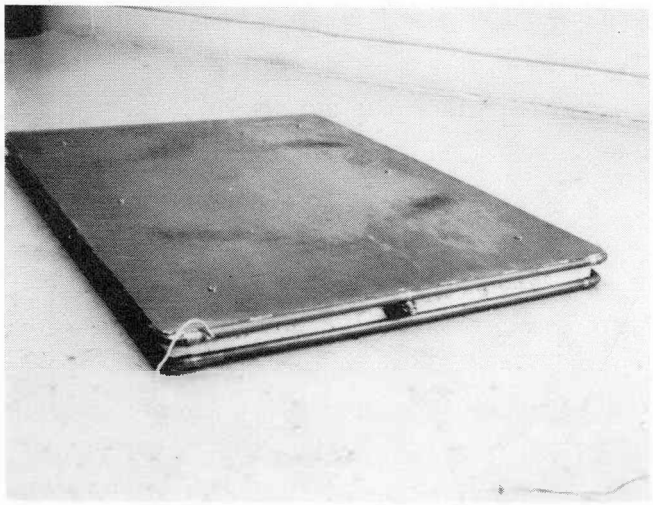

Figure 5.1 DISPLACEMENT CURRENT SENSOR

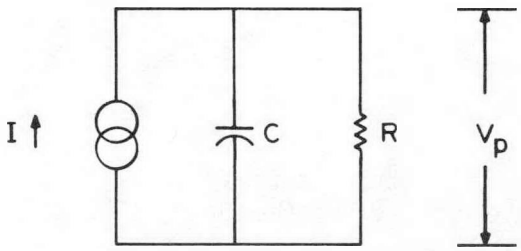

Figure 5.2 DISPLACEMENT CURRENT SENSOR EQUIVALENT CIRCUIT

Thus, the voltage sensed at the output of the displacement current probe is approximately 46 dB greater than the voltage which would appear across the pacemaker input for the same field strength and frequency.

It was of interest to insure the recovery of frequency components in the electric field to as high a frequency as possible. As will be noted in later discussion, our recording medium was limited to the range of 20-30 kHz. Figure 5.2 shows the equivalent circuit of the displacement current sensor. Here, the resistance, R, is the resistance placed between the plates, and the capacity, C, is the effective capacity between the plates. Using the effective area of the plates determined in the electric field facility, the capacitance of the plates was determined to be approximately 160 pf. From the equivalent circuit of Figure 5.2, and the value of resistance of 10 kΩ which was used, it was determined that the voltage output, V_p, deviates from the ideal value of IR by only 4 percent at a frequency of 30 kHz.

MAGNETIC FIELD SENSOR

As noted in Section 4, the magnetic field induces a voltage into an implanted pacemaker by means of the loop formed by the pacemaker lead and the associated return path through the body. The pacemaker senses this open circuit voltage. Thus, a sensor in which the open circuit voltage across a loop is sensed will respond in a similar manner to the pacemaker pickup in the body due to the magnetic field. Figure 5.3 shows a photograph of the loop probe fabricated for use on this program. In order to insure a measurement sensitivity greater than the loop formed in the body by the pacemaker lead, a multi-turn loop of eleven turns was used. The loop area was approximately 0.2 m^2. The loop was electrostatically shielded to prevent the loop sensor from responding to the co-existing electric field.

The loop was calibrated by use of a Helmholtz coil. Over the frequency range of 100 Hz to 10,000 Hz, where the calibration was performed, the loop probe response was nearly ideal, with a turns-area product of 2.133×10^4 cm^2. Using this effective area in Eq. 5-6 for the voltage induced in a loop of effective area, A, by a magnetic flux density, B, in gauss,

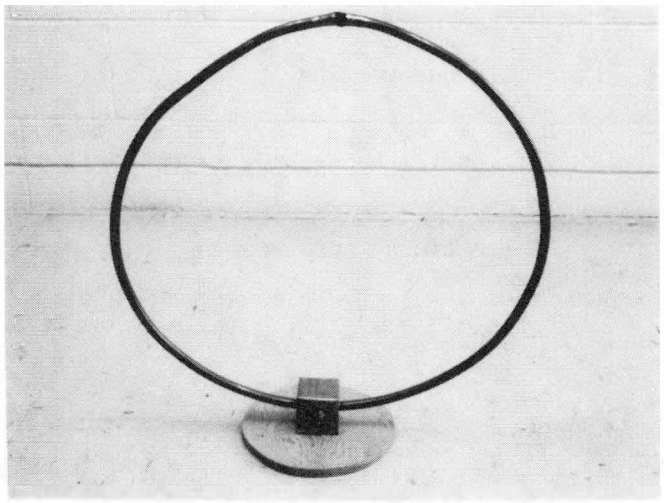

Figure 5.3 LOOP PROBE

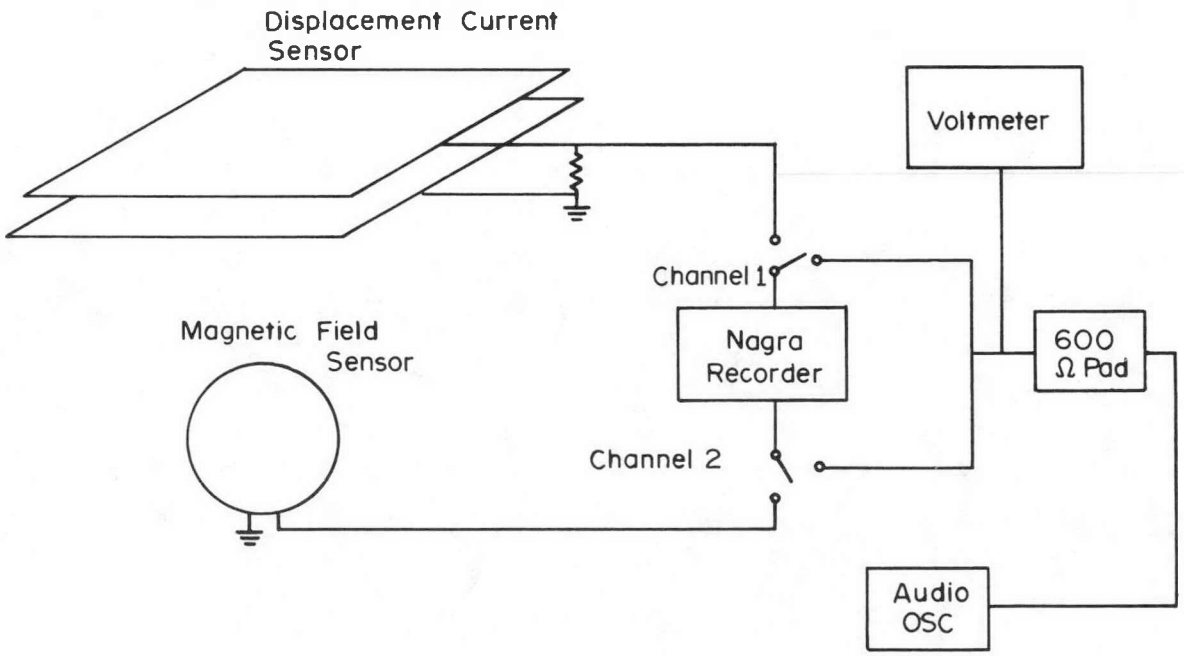

Figure 5.4 FIELD MEASUREMENT CONFIGURATION

$$V'_p = 2\pi f\ BA \times 10^{-8} \qquad (5\text{-}6)$$

at a frequency, f, in Hertz, it is found that the magnetic field induced probe voltage is

$$V'_p = 1.34 \times 10^{-3}\ fB \quad . \qquad (5\text{-}7)$$

The ratio of the voltage sensed by the magnetic field sensor to that anticipated in an implanted pacemaker with a 210 cm^2 effective loop area as given in Eq. 4-9, is

$$\frac{V'_p}{V_{ab}} = 10^2 \quad . \qquad (5\text{-}8)$$

Thus, the loop sensor will receive a signal which is 40 dB larger than anticipated for an implanted pacemaker for the same magnetic field density and frequency.

MEASUREMENT SYSTEM

The general configuration for the measurements made in the field are as shown in Figure 5.4. This figure shows the displacement current sensor and the magnetic field sensor, the tape recorder for recording the real time waveforms sensed by these field probes and the associated instrumentation necessary to provide a calibration of the recorded signal magnitudes. The tape recorder used to store the sensed signals was a Nagra Scientific Recorder Model IV-SJ. This recorder is battery operated. Pertinent specifications of the recorder are shown in Table 5.1. The Nagra recorder is equipped with a peak indicating meter and input attenuators on each channel to adjust the level of the input signal to the tape recording mechanism.

Prior to measurements in the field, tests were performed on the recorder to determine the input record level for acceptable harmonic distortion in the

Table 5.1

SPECIFICATIONS OF NAGRA MODEL IV-SJ TAPE RECORDER

Direct Record Input Impedance:	100 K	
Frequency Response:	15 ips	25 Hz to 35 kHz $\pm$ 1 dB
	7.5 ips	25 Hz to 20 kHz $\pm$ 1 dB
Wow and Flutter -- Unweighted rms:	15 ips	$\pm$ 0.06%
	7.5 ips	$\pm$ 0.08%
Crosstalk Attenuation:	at 1 kHz	$\geq$ 60 dB
	at 10 kHz	$\geq$ 50 dB
Signal to Noise Ratio:	15 ips	57 dB
	7.5 ips	60 dB
Phase Fluctuation Between Tracks:	at 7.5 ips ~~and 10 kHz~~	+ 12^{o}
Input Attenuator, Each Channel:	0-100 dB in	1 dB steps
	overall accuracy	$\pm$ 0.1 dB

recorder. It was found that if the peak signal level was maintained at 10 dB or more below the maximum peak recording level indication on the meter, the harmonics produced by the record/playback process were at least 50 dB down from the fundamental.

Prior to recording the signals sensed by the field probes, a calibration tone was placed on each channel of the recorder, using the setup shown in Figure 5.4. The level of the calibration tone was adjusted to be approximately 10 dB below the maximum peak level on the record meter. The voltmeter provided an indication of the absolute magnitude of the calibration tone. The absolute level of the calibration tone input was noted for each recording that was made. The procedures used in the bench testing of pacemakers made use of the calibration tone on playback to provide an absolute reference level for the signals recorded from the two field sensors.

Section 6

MEASUREMENT OF FIELDS ASSOCIATED WITH BPA CELILO HVDC CONVERTER TERMINAL

Measurements were made of the ac components of electric and magnetic fields at various locations within the Celilo HVDC terminal, located at the Dalles, Oregon, and at a representative location along one of the 230 kV ac feed lines to the terminal, and the dc line from the terminal. The following paragraphs describe the salient features of the Celilo facility ; identify the sites where measurements were made; and provide representative spectral and temporal data obtained at these sites.

DESCRIPTION OF CELILO HVDC FACILITY

Celilo is an ac-dc converter station on the Columbia River in Oregon. Direct current power is transmitted between Celilo and Sylmar, its counterpart in southern California, to form the first major dc tie in the United States. This converter station is presently the world's largest, capable of transmitting almost the total output of Bonneville and the Dalles dams.

The dc system is a bipolar system, consisting of two conductors (poles), one working at + 400 kV and the other at -400 kV. Normally, with both poles in operation, current flows north to south in one conductor, and south to north in the other. The Celilo terminal has a capacity of 1440 megawatts. Each pole or dc conductor is fed by three converter groups connected in series. Each converter group consists of a bridge of six mercury arc valves and a bypass valve, which permits a group to be cut out of service for short periods of time. The currents in the two poles are kept equal so that there is no unbalanced ground current for loss of one or two groups in each pole. Loss of one converter group will result in reduction in voltage for that pole to two-thirds. Similarly, loss of two groups in one pole will result in reduction in voltage for that pole to one-third of rated voltage.

When the terminal is converting to dc, two 230-kV three phase lines from the Big Eddy ac substation about a mile away, carry power to the Celilo terminal. Under normal operation, each ac line supplies a bus section associated with one pole of the dc transmission line. Each converter group is a three phase full wave bridge circuit using two mercury arc valves per phase to switch the current.

In the process of ac to dc conversion, harmonic currents are generated by the converter terminal. To prevent these harmonics from spreading into the BPA grid system and causing telephone interference, harmonic filters are incorporated as a part of the Celilo facility. These filters provide a low impedance path to ground for some of the major harmonic frequency components.

Characteristic harmonic currents generated by the converter are the fifth, seventh, eleventh, thirteenth, and higher frequency harmonics, following the law ($6n \pm 1$, where n is an integer). Through the use of an equal number of Y and ∇ connected converter transformer banks, those harmonics corresponding to odd-numbered values of n will be cancelled out. However, when one valve group is out of service, the fifth and seventh harmonics do not cancel; therefore, fifth and seventh harmonic filters are provided. Since the eleventh and thirteenth harmonics are not cancelled due to the transformer connections, filters for these harmonics are provided on each 230 kV bus section within the Celilo terminal. The fifth and seventh harmonic cancellation, as well as filters for these harmonics, is at the Big Eddy substation.

Each 230 kV bus section also has broadly tuned filters for the higher harmonics. Also, untuned shunt capacitors are provided for power factor correction, and these are also helpful and reduce the harmonics, particularly at the higher frequencies.

The dc voltage produced by the valve groups is not smooth, and contains a range of harmonics. The resulting harmonic voltages and currents on the dc line are limited by a dc reactor connected in series with each pole.

The dc smoothing reactor cannot limit the harmonic currents in the dc line to an acceptable level by itself. To further reduce telephone interference that may occur, a sixth harmonic filter and a high pass filter have been provided between each pole and neutral.

MEASUREMENT SITES

It was desired to perform field measurements at representative sites within the Celilo terminal, and beneath both the ac and dc lines outside the terminal. Figure 6.1 shows a simple line drawing that is useful in identifying the sites at which measurements were made, and presenting the rationale for the choice of sites. This figure depicts one of the three phase 230 kV ac lines which feed the Celilo terminal. This ac line feeds the three converter groups associated with one of the dc poles. As discussed in the previous section, filters are provided on this ac line to minimize the harmonics generated by the conversion process. The ac side harmonic filters are shown as a block on this drawing.

On the dc side, the three converter groups are connected in series as shown. The harmonic filters on the dc side are shown functionally as a block in Figure 6.1. This drawing shows only one dc pole and one ac line feeding the station. A duplicate of this arrangement exists to produce dc of the opposite polarity with respect to neutral, thus providing the full 800 kV line-to-line dc output voltage. However, for the purpose of functionally identifying the location of test sites, only one dc pole and its associated ac supply are shown.

Measurements within the Celilo terminal facility were conducted at five different sites. These sites are identified in Figure 6.1 by small circles. These sites are numbered in order of the sequence in which the measurements were made. Figure 6.2 shows the measurement sites #1 through #5 spotted on a plot plan of the Celilo converter station.

Site #1 was beneath the ac line, between the converter groups and the ac side harmonic filter group. It was anticipated that the 60 Hz and harmonic current components should be maximum in this section of line. A view of measurement site #1 is shown in Figure 6.3.

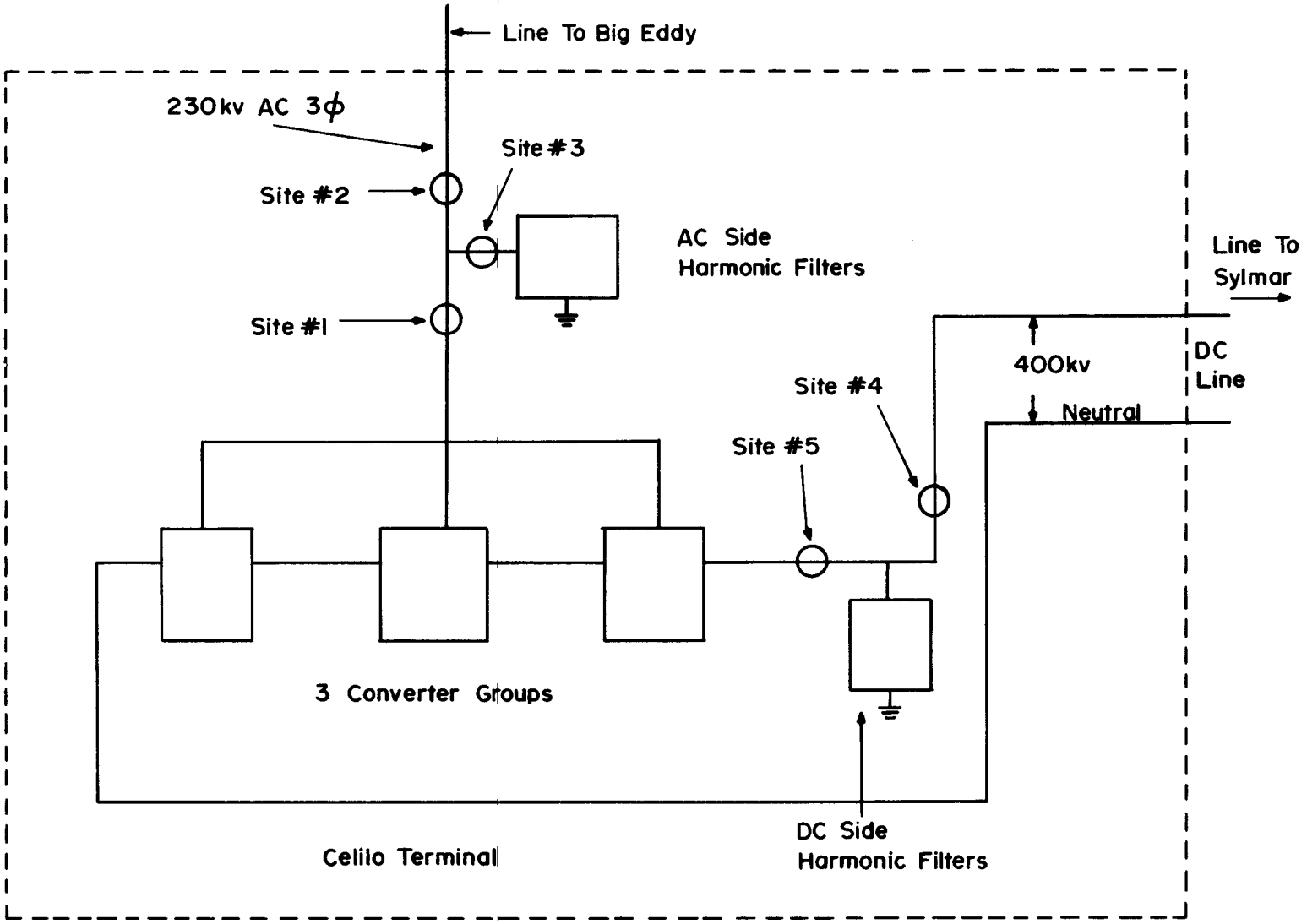

Figure 6.1 FUNCTIONAL LOCATION OF MEASUREMENT SITES

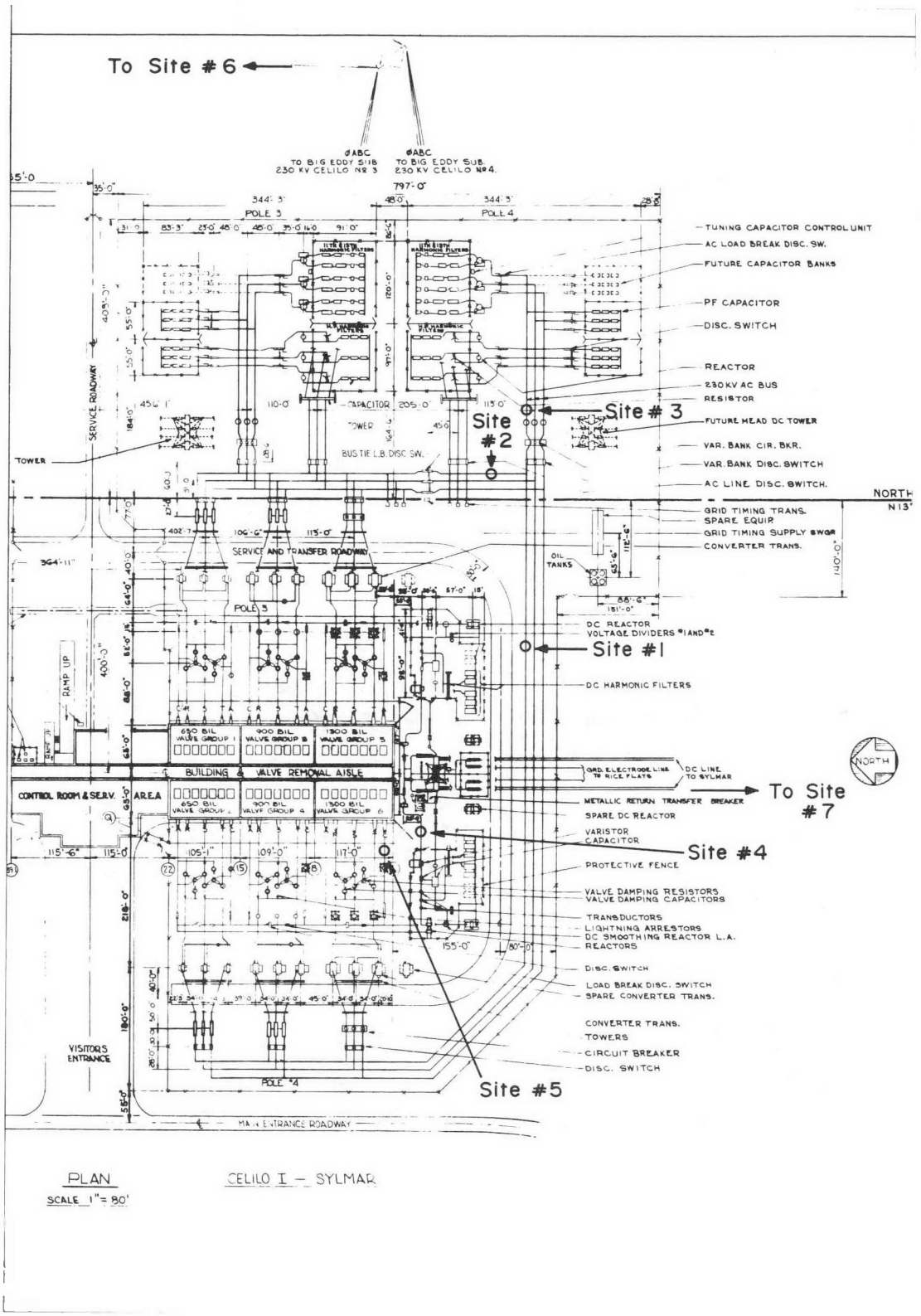

Figure 6.2 CELILO FACILITY PLAN VIEW

Site #2 was beneath the ac line on the ac substation side of the filter group. Figure 6.4 shows a view of this measurement site. In this section of line, the higher harmonic currents were anticipated to be reduced from the levels of site #1, due to the shunting effect of the filter group.

Site #3 was beneath the ac line section that feeds into the ac-side filter group. Figure 6.5 shows a view of this site. The higher harmonic currents flow toward the low impedance filters in this section of line. It was anticipated that this section of line would produce fields with a high ratio of harmonic to 60 Hz component, since the 60 Hz current flow to the filter group is relatively low.

Due to the different amount of harmonic current, relative to 60 Hz current which flows in the transmission lines at sites #1 through #3, it was anticipated that the magnetic field time history and spectrum would be quite different at these three sites. However, since the transmission lines at all three sites have a common node, the electric fields should be quite similar at these three sites.

Site #4 was beneath the dc line on the output side of the dc harmonic filter group. Figure 6.6 shows a view of this site. At this point, the effect of the filters in cleaning up the dc line should be evident. In contrast, site #5 was beneath the dc line between the converter groups and the dc filters. Thus, the harmonics at site #5 were expected to be as large or larger than at any point along the converter group chain.

Measurement site #6 was made on the 230 kV line #3 between towers #3 and #4, beneath the C phase on the east shoulder of the road where the transmission line crossed over the road. Test site #7 was beneath the Celilo-Sylmar dc line, midway between towers #3 and #4. This site should provide measurements representative of other sites along the Pacific HVDC intertie. Figure 6.7 shows a view of this site.

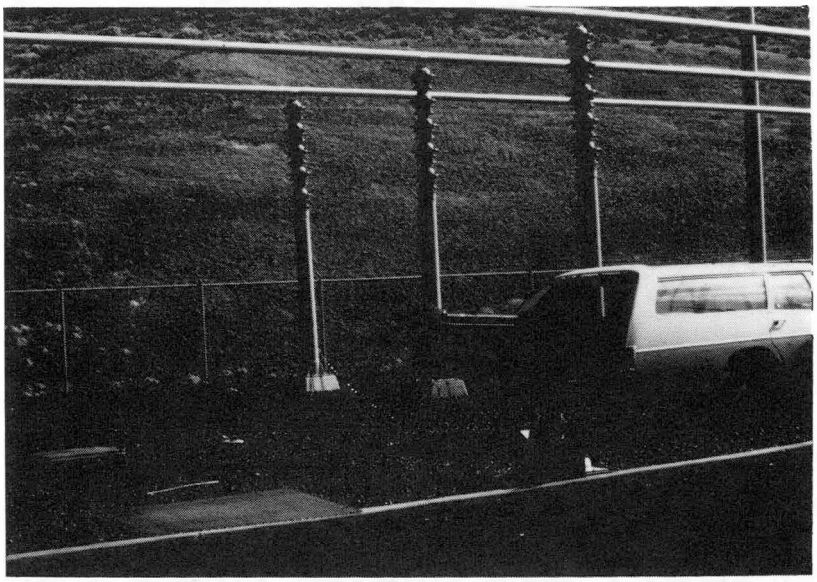

Figure 6.3 PHOTOGRAPH OF SENSORS AT SITE 1

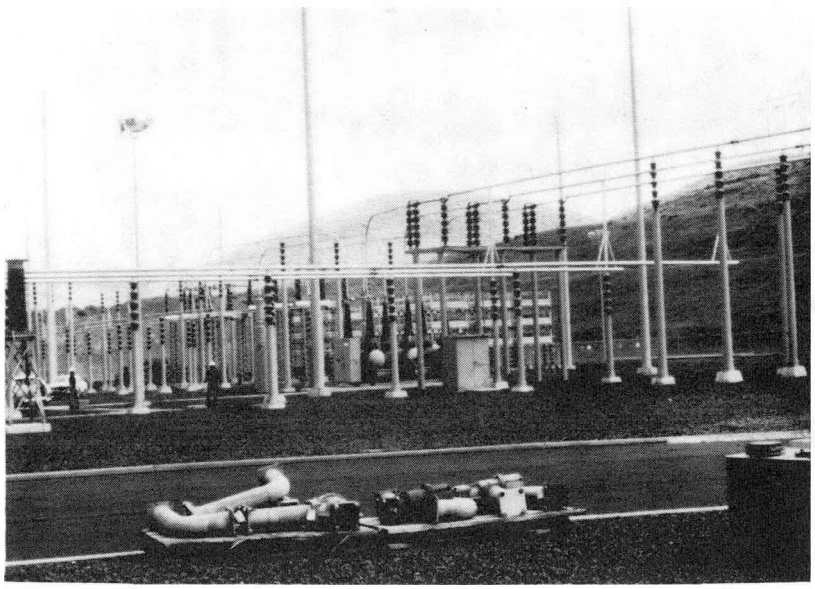

Figure 6.4 VIEW OF MEASUREMENT SITE 2

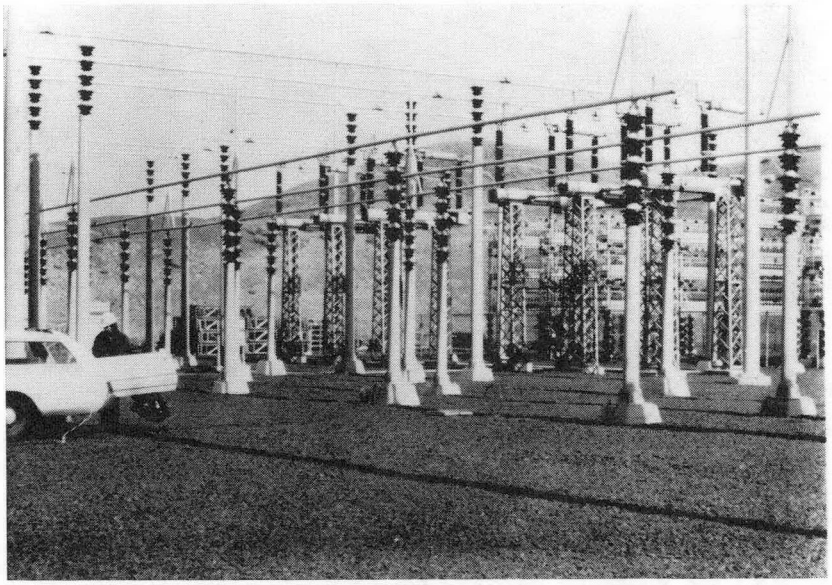

Figure 6.5 VIEW OF MEASUREMENT SITE 3

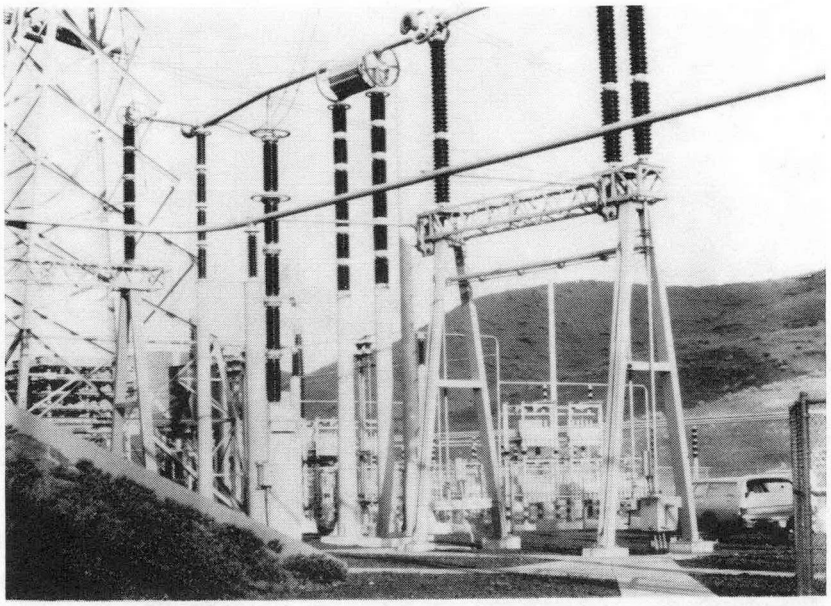

Figure 6.6 VIEW OF MEASUREMENT SITE 4

ELECTRIC AND MAGNETIC FIELDS AT MEASUREMENT SITES

In this section, selected samples of the data obtained at each test site will be presented. At each test site, the real time output from the $\dot{D}$ and the $\dot{B}$ sensors were recorded on the Nagra tape recorder for later use in pacemaker testing. In addition, spectrum analyzer displays of the output voltage from the two sensors were recorded at most sites, as was the real time voltage output from the sensors, which was displayed on an oscilloscope.

The spectral output from the two sensors, as displayed on the spectrum analyzer, requires some interpretation in order to relate to the magnetic flux density, or the electric field intensity at the various harmonic frequencies. As was described in Section 5, the voltage output from the parallel plate sensor is proportional to the derivative of the electric field intensity, or $\dot{E}$. Similarly, for the loop sensor, the voltage output is proportional to the derivative of the magnetic flux density, or $\dot{B}$. Thus, the output voltage from these sensors is proportional to the frequency of the harmonic component of the field.

The spectrum analyzer that was used displays the magnitude of the various spectral components of the sensor output voltage on a decibel scale, which is referenced to one volt. Each major ordinate division on the spectrum analyzer output display is ten decibels, and the full scale value is a multiple of 10 dB referenced to one volt. Thus, for example, full scale on the spectrum analyzer display might be -10 dBV or -20 dBV, or some other value which was appropriate for providing a good display of the spectrum. Figure 6.8 presents a representative spectrum display of the voltage output from the $\dot{E}$ sensor. Full scale in this display is -10 dBV (i.e., ten decibels below one volt). The amplitude display is 10 dB per division, and the abscissa or frequency scale is 200 Hz per division.

The magnitude of the electric field component at the various harmonic frequencies cannot be ascertained directly from this spectral display. However, Figures 6.9 and 6.10 present nomograms which can be used to determine the magnitude of the electric field component or the magnetic flux density component

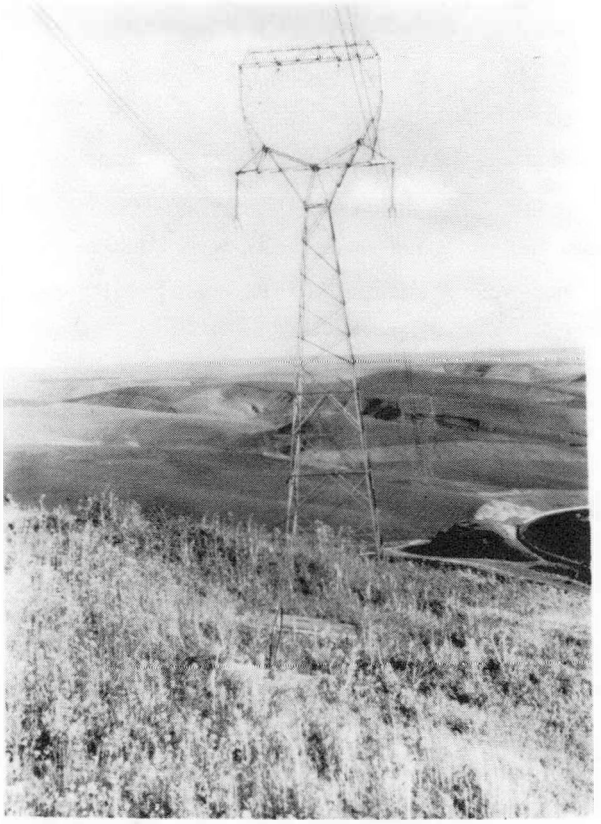

Figure 6.7 VIEW OF MEASUREMENT SITE 7

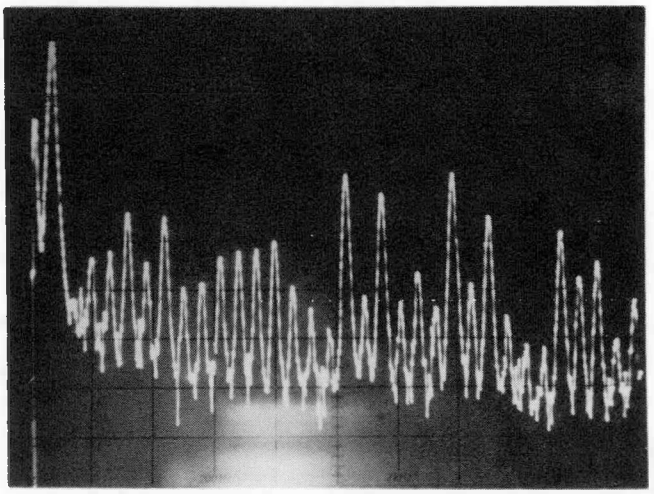

Full Scale -10 dB V
10 dB/division
200 Hz/division

Figure 6.8 REPRESENTATIVE SPECTRUM DISPLAY OF $\dot{E}$ SENSOR VOLTAGE OUTPUT

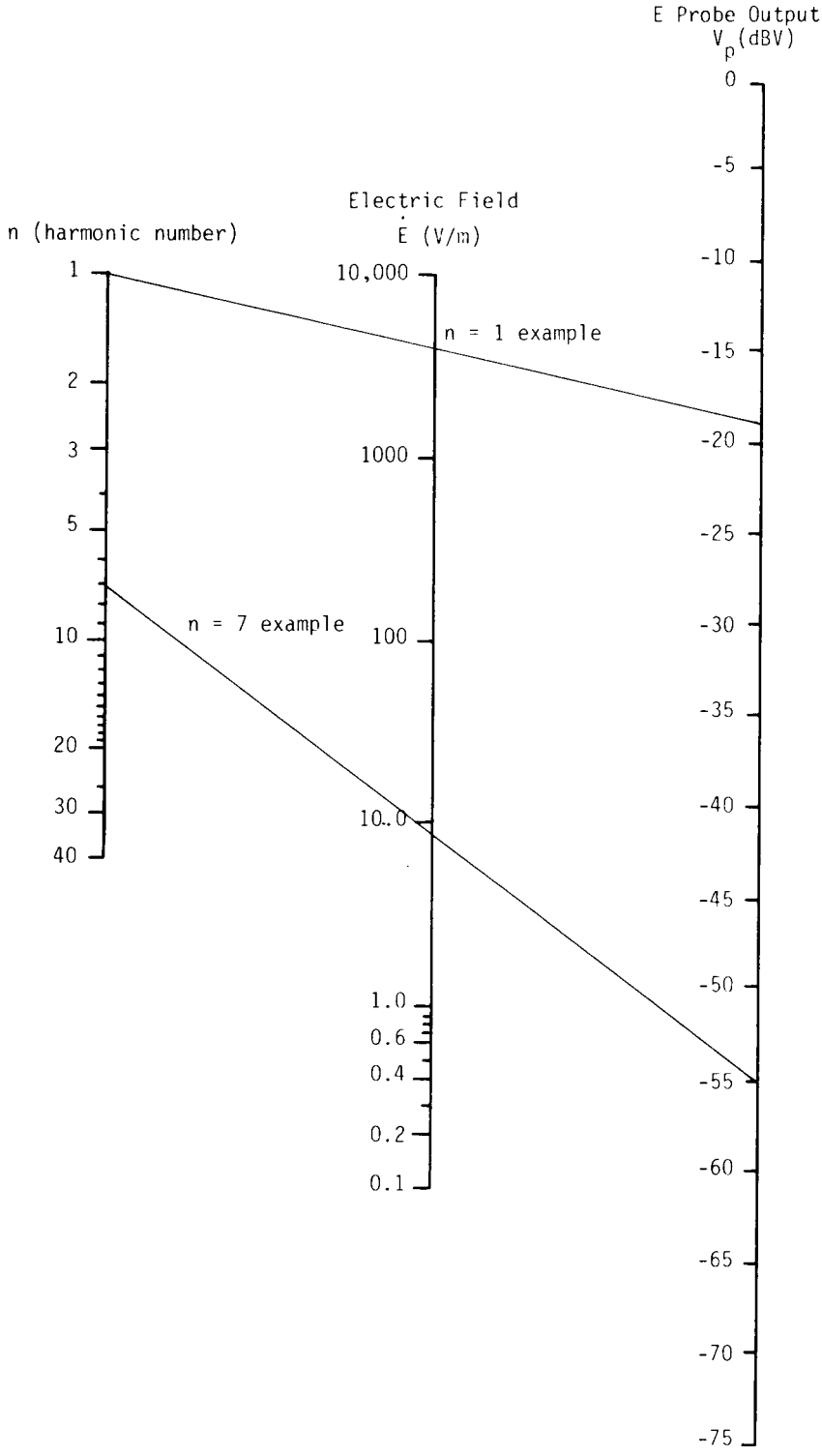

Figure 6.9 NOMOGRAM FOR RELATING HARMONIC COMPONENT OF $\dot{E}$ SENSOR OUTPUT TO ELECTRIC FIELD INTENSITY

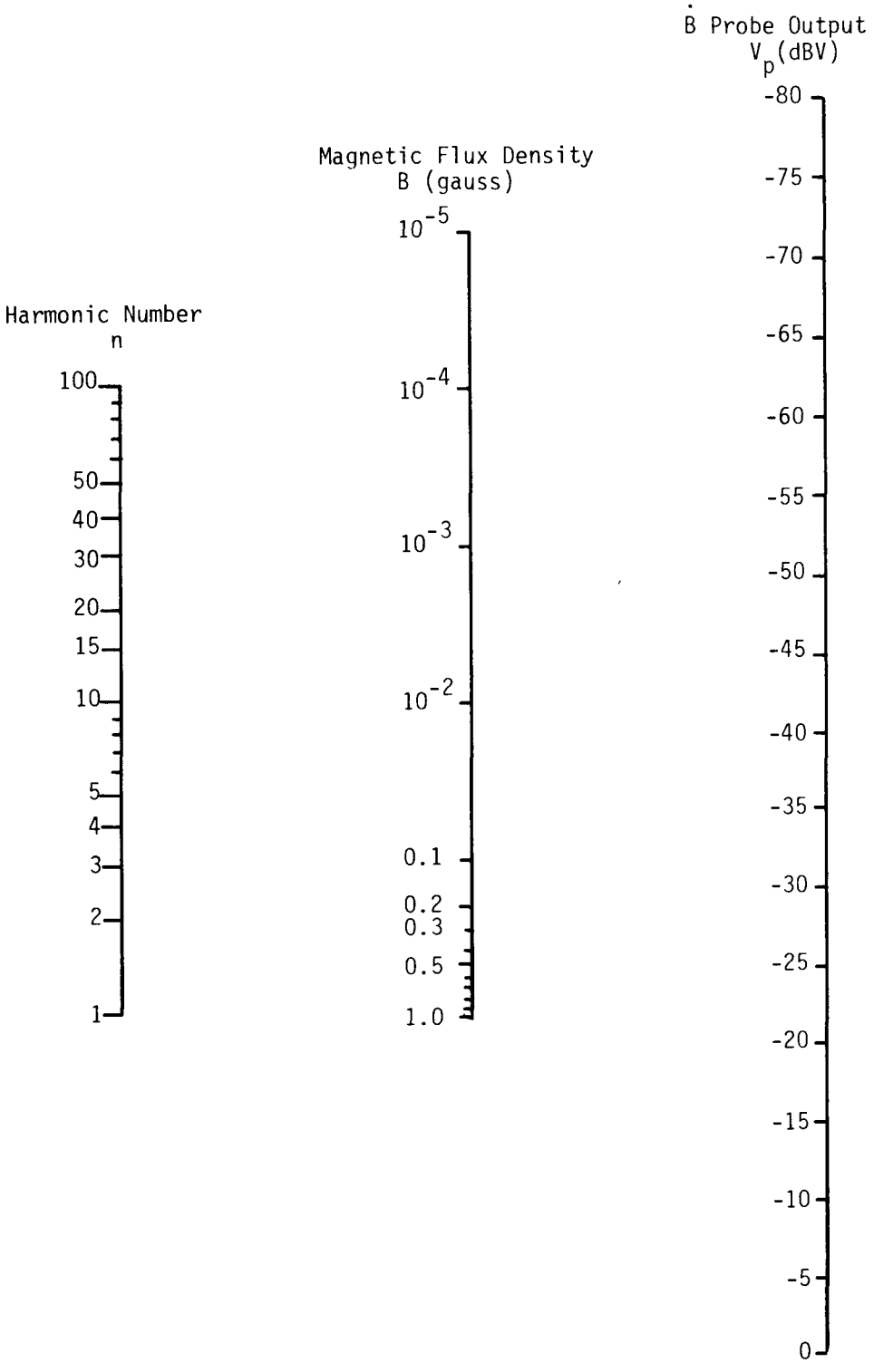

Figure 6.10 NOMOGRAM FOR RELATING HARMONIC COMPONENT OF $\dot{B}$ SENSOR OUTPUT TO MAGNETIC FLUX DENSITY

at the various harmonic frequencies, from the spectral displays of the output voltages from the $\dot{E}$ or $\dot{B}$ sensors, respectively.

To use these nomograms, the harmonic number of interest must be determined from the spectral display. Also, the amplitude of this harmonic component must be determined from the spectral display. The harmonic amplitude from the spectral display is in terms of dB relative to a volt, or dBV. An example will be given here to illustrate the use of these nomograms by reference to the $\dot{E}$ spectrum shown in Figure 6.8.

From Figure 6.8 it is seen that the 60 Hz component is approximately -19 dBV. The harmonic number of the 60 Hz component is one. Using the nomogram of Figure 6.9, draw a straight line between the value 1 on the harmonic number scale and minus 19 in the V_p scale. This line crosses the electric field scale at approximately 3600 volts per meter.

Similarly, from the spectrum in Figure 6.8, it is seen that the seventh harmonic component is approximately -55 dBV. Again using the nomogram of Figure 6.9, a line drawn between n = 7 on the n scale, and V_p = -55 on the V_p scale, crosses the electric field scale at approximately 9 V/m. The same procedure as illustrated here with the spectral display of the $\dot{E}$ sensor, can be applied to determining the magnetic flux density of spectral components from the $\dot{B}$ sensor, by use of the nomogram of Figure 6.10.

Representative $\dot{E}$ and $\dot{B}$ spectra and voltage wave shapes obtained at the various test sites are presented in Appendix A. At this point, some of the salient aspects of the measurements and results will be discussed. Reference will be made to the figures in Appendix A where necessary.

At site #1, some initial measurements were made to determine how the field varied with position relative to the 230 kV line under which measurements were made, and to check out the performance of the sensors. The $\dot{E}$ sensor had been calibrated in the laboratory, using the IITRI E-field facility. For the

calibration, the ground plate of the $\dot{E}$ sensor was directly connected to the ground plate of the electric field facility. Since no guard ring was used with the $\dot{E}$ sensor, it was desired to establish if the effective area of this sensor differed when working against a large metallic ground as compared to working against a real ground as in the field.

Within the Celilo terminal complex, a ground grid exists to which all metallic items are tied. The ground plate of the $\dot{E}$ sensor was connected to this ground grid, by means of a wire which was run to the closest metallic item and its associated ground strap. To determine the adequacy of this ground, a ground stake was also driven near the $\dot{E}$ sensor and connected to the sensor ground plate. It was found that connecting or disconnecting the $\dot{E}$ ground plate from the ground stake made no difference in the measured field level. In addition, a test was performed by placing a large metal sheet beneath the $\dot{E}$ sensor. This sheet was grounded to the ground stake and to the facility ground grid. Again, no significant difference in the sensed field level was obtained whether or not the large metallic plate was under the $\dot{E}$ sensor. Thus measurements at other sites within the facility were made by running a wire from the $\dot{E}$ sensor ground plate to the closest facility ground grid attachment point.

Initially, the $\dot{E}$ sensor was moved along a line normal to the direction of the transmission line to find the point of highest field intensity. It was found that the sensor output maximized when the sensor was located approximately one meter outside of the outer phase of the 230 kV line at site #1. Thus measurements at sites 1, 2, and 3, which were beneath the 230 kV ac line within the facility, were made at a location which was approximately one meter outside of the outer phase and nominally mid-span between supporting posts for the line.

Measurements made at sites 1, 2, and 3, which are associated with the 230 kV ac bus within the facility are presented in Figures A-1, A-2, and A-3 in Appendix A. These figures show a spectral presentation of the voltage output from both the $\dot{E}$ sensor and the $\dot{B}$ sensor. Also shown are time waveforms of the outputs from the sensors. Comparison of the $\dot{E}$ sensor output spectrum for these three measurement sites show that over the lower frequency range, i.e., below

2000 Hz, the electric field spectrum is virtually identical for all three sites. However, it is seen that the magnetic field spectral components differ somewhat from site to site due to the effect of the ac harmonic filters on the harmonic current flow in the line.

In the time history waveforms shown in Figures A.1 through A.3, it will be noticed that both the $\dot{E}$ sensor and the $\dot{B}$ sensor voltage time waveforms contained transient spikes. These transient spikes are damped waveforms which, in some instances, had primary frequency components above the bandwidth of the audio recording instrumentation used. Figures 6.11 and 6.12 show examples of the ringing transients from the $\dot{E}$ sensor and the $\dot{B}$ sensor, respectively.

Figures A.4 through A.7 show representative spectra and real-time waveforms obtained with the $\dot{E}$ and $\dot{B}$ sensors at sites 4 and 5, which were associated with the dc conductors in the converter station.

Figure A.8 shows representative spectra and waveshapes obtained at site #6, which was beneath one of the 230 kV ac transmission lines that supply power to the converter terminal. At this site, an additional experiment was conducted to verify that all of the significant displacement current harmonic components that were being measured by the $\dot{E}$ sensor would indeed flow through a person. In addition, if the recorded signal from the sensor was to be validly employed for pacemaker testing, the relative amplitude of the harmonic components had to be the same for the sensor as for a human.

To verify the above factors, the spectral output from the $\dot{E}$ sensor alone was obtained. This is shown in Figure A.8. The $\dot{E}$ sensor output was then obtained with a man standing on top of the sensor top plate. For this condition, the sensor should primarily measure a signal proportional to the current flow through the man, since the effective area of the man was roughly 5 m^2, while the area of the sensor was approximately 0.86 m^2. The ratio of the areas should correlate quite closely to the ratio of the signals observed for the two conditions.

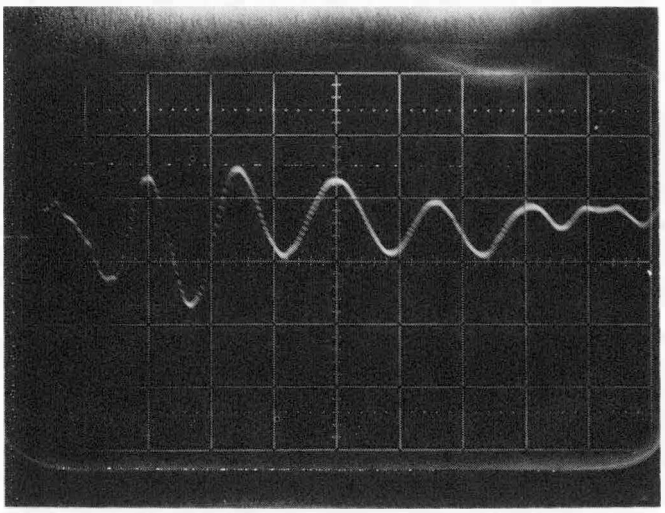

20 μs/division
0.1 V/division

Figure 6.11 HIGH FREQUENCY RINGING SEGMENT OF $\dot{E}$ SENSOR OUTPUT AT SITE 2

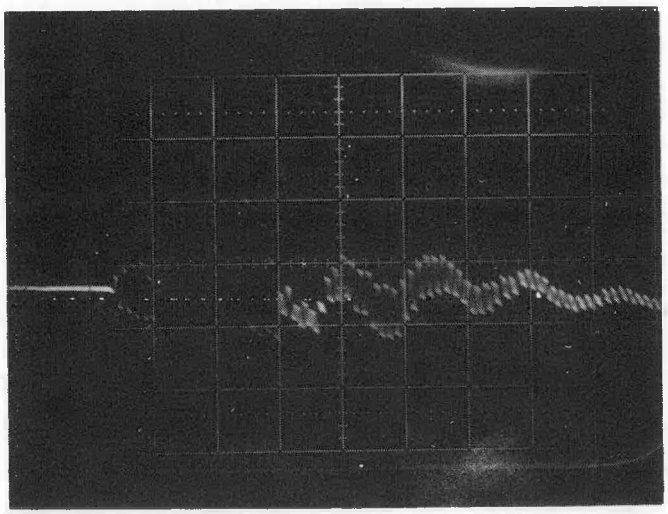

20 μs/division
0.2 V/division

Figure 6.12 HIGH FREQUENCY RINGING SEGMENT OF $\dot{B}$ SENSOR OUTPUT AT SITE 2

Figure 6.13 shows the spectral output from the $\dot{E}$ sensor with the man standing on top. The frequency scale for this spectrum is the same as for the sensor alone, which is shown in Figure A.8. However, for Figure 6.13, the full scale level is 0 dBV, while for the spectrum of Figure A.8, the full scale level is -20 dBV. The ratio of the areas is somewhat greater than 15 dB, while the spectral components of Figure 6.13 are approximately 18 dB larger than those of Figure A.8. It is felt that this agreement is quite adequate. In addition, it is seen that the harmonic component amplitudes relative to one another are the same for both figures. Thus, the $\dot{E}$ sensor output, when properly scaled to account for collection area, provides an adequate representation of human body current flow for the harmonic components of interest.

Representative waveforms and spectra obtained at site #7, beneath the dc transmission line, are shown in Figure A.9. It will be noted that the signals are lower at this site than the other sites tested.

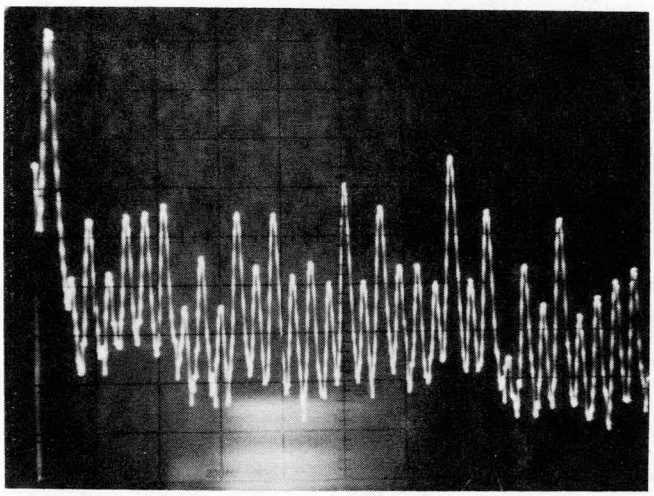

200 Hz/division
0 dBV Full Scale

Figure 6.13 $\dot{E}$ SENSOR OUTPUT WITH MAN STANDING ON TOP

Section 7

LABORATORY TESTING OF PACEMAKERS

The field measurements described in the previous section resulted in the production of magnetic tape recordings of real time voltage signals. These signals were proportional to the time derivative of the electric and magnetic fields, at selected locations associated with the Celilo HVDC facility.

In this section, the procedures and results of laboratory testing of representative pacemakers will be described. The objective of the pacemaker bench tests was to determine the performance of a group of representative production line pacemakers when subjected to interfering signals such as might be collected by the body of a person standing at typical locations within or near a HVDC terminal. The use of bench tests provides an indication of pacemaker response to body-collected interference signals without the necessity for human subject testing. The bench testing relied upon models for electric field pickup developed by Bridges and Frazier (1976) (1) and for magnetic field pickup developed by D.A. Miller (1971)(2). The bench testing to be reported here, utilized pacemaker input signals that represented the composite voltage which might be anticipated on a near worst-case basis from the combination of both the electric and magnetic field body pickup.

The following paragraphs describe the calibration and scaling procedures which relate the magnetic and electric field sensor signals, that were recorded on magnetic tape during the Celilo tests, to the voltages at the pacemaker input for bench testing. Also described are the test procedures and instrumentation used in the bench testing, as well as the results of these tests.

SCALING AND CALIBRATION OF TAPE RECORDED SIGNALS

In Section 5 it was shown that the $\dot{E}$ sensor used for the field testing resulted in an output voltage which was larger than the voltage anticipated to be developed across the input to an abdominally located monopolar pacemaker, with 15 cm

vertical electrode separation. For these conditions, the ratio of the probe voltage to pacemaker voltage was given in Eq. 5.5 as

$$\frac{V_p}{V_{ab}} = 2.07 \times 10^2 \qquad (7\text{-}1)$$

where V_p is the $\dot{E}$ probe voltage and V_{ab} is the voltage expected at an implanted pacemaker input for a well-grounded person standing with arms to side at the same location as the sensor.

In Section 5 it was also shown in Eq. 5-8 that the magnetic field sensor output voltage was greater by a factor of 10^2 than would be developed across an implanted pacemaker having an effective loop area of 210 cm^2.

Thus, in using the magnetically recorded real-time field signals for bench testing of pacemakers, it was necessary to reduce the $\dot{E}$ sensor by a factor of 2.07×10^2 (approximately 46 dB) and to reduce the $\dot{B}$ sensor signal by a factor of 10^2 (40 dB).

In order to appropriately scale the tape recorded data for use in bench testing, it was necessary to have a procedure that accounted for the gain of the record and playback process. The procedure that was used was to record a known-level calibration signal on each tape channel just prior to recording the sensor output signals. The gains of all components of the field measurement system remained fixed between the above two steps. In the bench tests, the playback gains were adjusted to provide the known calibration signal voltage level at the point in the test setup where the pacemaker under test would be connected. The detailed procedures used in the playback calibration are further discussed in the following paragraphs with reference to the bench test setup and procedures.

BENCH SETUP AND PROCEDURES

In discussing the procedures used for bench testing of pacemakers with the signals recorded from the $\dot{E}$ and $\dot{B}$ sensor outputs, the block diagram shown in

Figure 7.1 will be referenced. Figure 7.1 shows the block diagram of the test setup used for the bench tests.

As previously noted, the signals from the $\dot{E}$ and $\dot{B}$ sensors were each recorded on a separate track of the tape recorder. However, the two signals were recorded simultaneously. Also, as noted above, a known-level calibration signal was recorded on each channel prior to recording the sensor output signals at each test site.

The procedure used in the bench test to establish the voltage at the pacemaker input at 46 dB below the $\dot{E}$ sensor output and 40 dB below the $\dot{B}$ sensor output included the following series of steps:

1. Pad #3 was set for 5 dB with the pacemaker disconnected. This initial step insured that the impedance at the point where the voltage was measured was 600 ohms.

2. Pad #1 was adjusted until the Channel 1 calibration tone output as measured by the voltmeter shown, was equal to the level of the Channel 1 calibration signal recorded during the field test.

3. Step 2 above was repeated for Channel 2, using Pad #2.

4. After the above three steps, an additional 6 dB was added to Pad #1 and 40 dB was added to Pad #3.

Steps 1 through 3 above insured that the sensor signal output levels which were recorded in the field test, were the same as would appear at the pacemaker input terminal (Point A in Figure 7.1). Thus, these steps corrected for recorded playback gains.

Step 4 above resulted in the signal level at Point A (where the pacemaker was to be connected) being 46 dB below the $\dot{E}$ sensor output and 40 dB below the $\dot{B}$ sensor output. Under these conditions, the signal at Point A from Channel 1 was equivalent to that which would be developed across the input to an abdominal monopolar pacemaker with 15 cm electrode separation due to electric field excitation of the patient. The signal at Point A from Channel 2 was equivalent

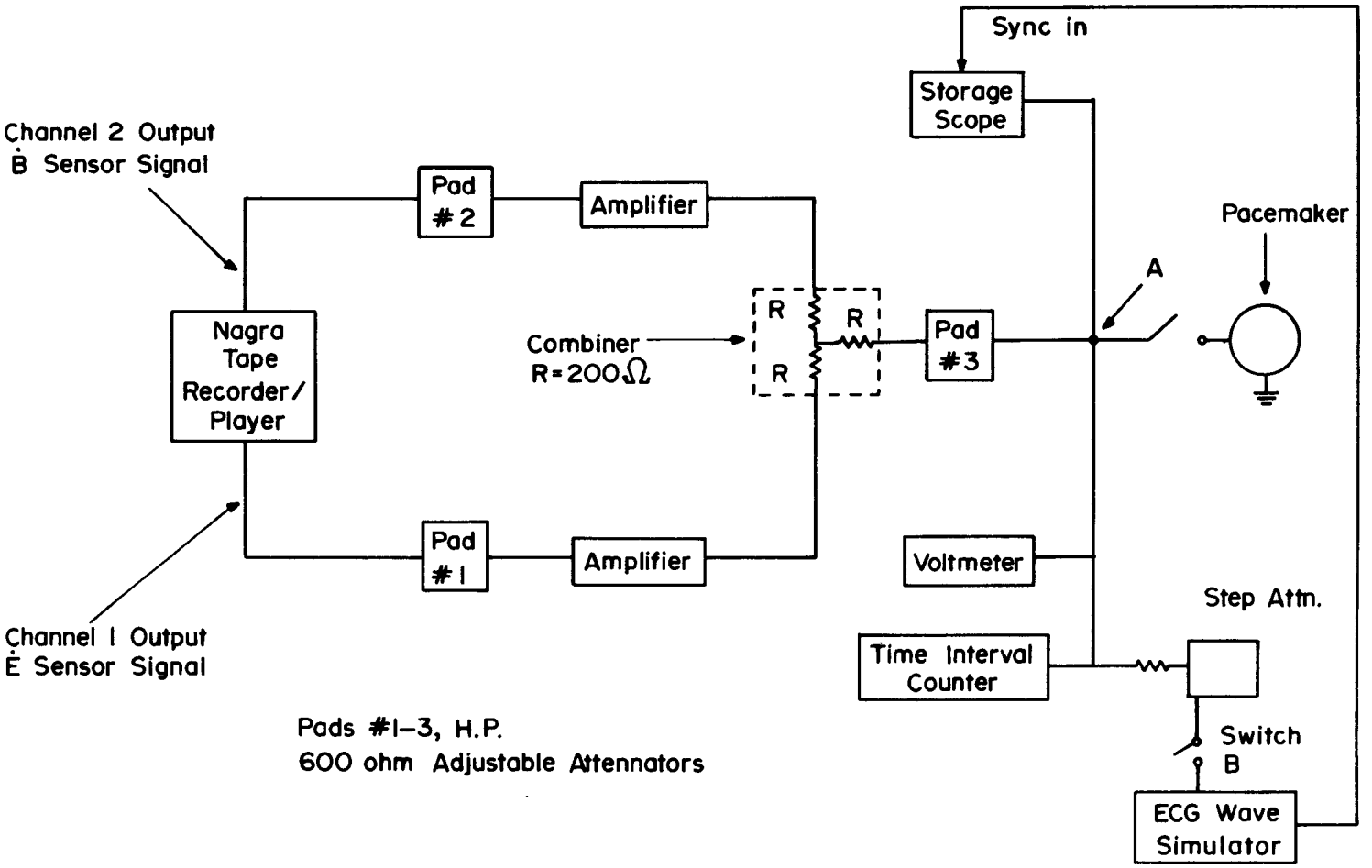

Figure 7.1 TEST SETUP FOR BENCH TESTS

to that which would be developed across a 210 cm^2 pacemaker electrode loop. The combined voltage at Point A, with signals from both playback channels, represented the total voltage which would be seen by the pacemaker due to the combined electric and magnetic field. At this point in the test procedure, the setting of Pad #3 was 45 dB. During the testing, the attenuation of this pad was both increased and decreased. However, the above condition, i.e., 46 dB in Pad #3 is referred to as the reference condition.

The pacemakers were tested under two simulated ECG waveform conditions. The first condition was with a simulated ECG signal applied to the pacemaker. The second condition was with no simulated ECG signal applied. The simulated ECG signal used for these tests, as would be measured at the pacemaker input, is shown in Figure 7.2.

All but one of the pacemakers tested were of the R-wave inhibited type. For these pacemakers, with a simulated ECG signal and no interference applied, the pacemaker did not produce pulses. This condition simulates the case where the patient's heart is normally beating. Under this condition the pacemaker should be inhibited. If an interference signal is added to the pacemaker input when an ECG signal is present, the pacemaker will revert to the asynchronous mode of operation when the interference signal becomes sufficiently large.

When no ECG signal is applied to the pacemaker, the pacemaker should produce pulses at its design rate. This condition simulates the case where the patient is totally dependent on the pacemaker. Under this condition, the addition of an interference signal should not materially alter the operation of the pacemaker. Interference induced rate changes to less than 50 beats per minute, or greater than 120 beats per minute, are generally considered to be undesirable.

The one pacemaker tested which was not an R-wave inhibited unit was an R-wave synchronous type. This type pacemaker behaves essentially the same as the inhibited type with the exception that rather than being inhibited by an ECG

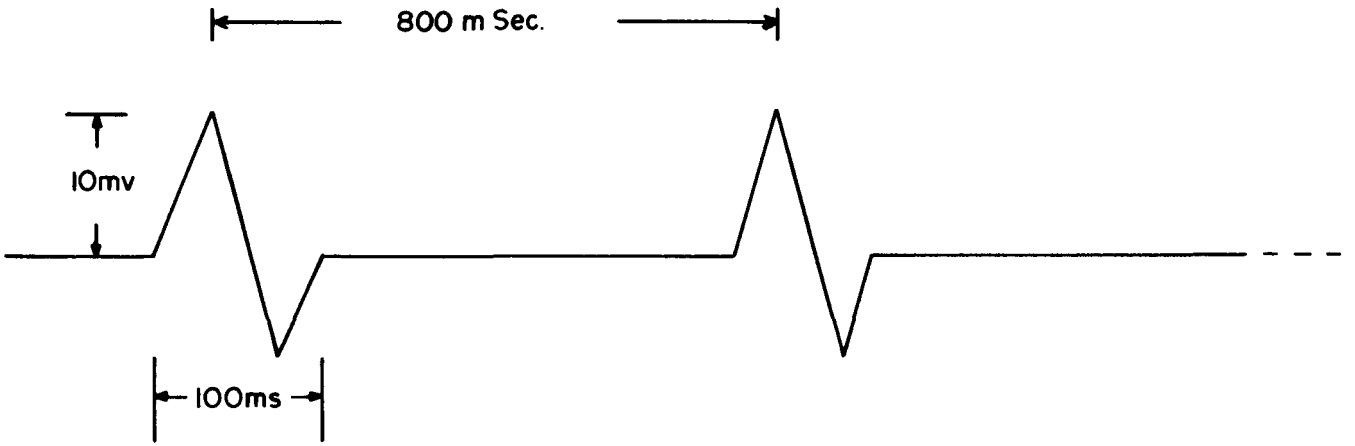

Figure 7.2 SIMULATED ECG SIGNAL

waveform, the pacemaker produces pulses that are synchronized in time to the R-wave of the ECG signal.

The testing of the pacemakers, either with or without a simulated ECG signal, was performed by varying the total interference voltage at the pacemaker. The total interference to the pacemaker, i.e., the combined output from the $\dot{E}$ and $\dot{B}$ channels at Point A of Figure 7.1, was varied in 1 dB steps by changing the attenuation of Pad #3. The settingsof this pad which produced changes in the pacemaker operation from the "no interference" condition were noted.

Changes in the setting of Pad #3, from the reference condition of 45 dB, relate to either more or less than the measured field being required to cause observable interference to the tested pacemaker. For example, consider the case of a pacemaker being tested with an applied ECG signal. Assume the pacemaker is inhibited (does not sense interference) with the reference level of interference (Pad #3 at 45 dB) from a particular field measurement site, but reverts when the interference level is increased by 6 dB. This means that the fields at the measurement site could be up to twice as strong as were measured before the implanted pacemaker would revert.

Each of the six pacemakers, both with and without a simulated ECG signal, were tested to the combined $\dot{E}$ and $\dot{B}$ interference from each of the seven field measurement sites.

The specific procedure followed after the four calibration steps noted above was:

1. Connect pacemaker to Point A without simulated ECG and measure pacemaker output rate with no output from tape recorder.

2. Set Pad #3 to 55 dB (a factor of 3 less signal than at measurement site), turn on tape playback and note any deviation of pacemaker performance from "no interference" condition.

3. Increase interference signal at pacemaker in 1 db steps noting any changes in pacemaker rate response at each signal level. Continue this sequence until all attenuation is removed from Pad #3 (with no attenuation in Pad #3, the interference level at the pacemaker input is approximately a factor of 178 greater than would be sensed by the pacemaker with the assumed implant conditions and the patient standing well-grounded at the field measurement site).

4. Repeat the above three steps with simulated ECG supplied to pacemaker.

RESULTS OF PACEMAKER BENCH TESTING

This section presents the results of testing the six pacemakers to the signals recorded at each of the seven measurement sites associated with the Celilio HVDC facility.

For the test condition of no simulated ECG signal to the pacemakers, five of the pacemakers continued to pulse at their design rate for all levels of interference tested (up to 178 times the reference interference signal level). The sixth pacemaker evidenced occasional skipped pulses when subjected to the interference signal measured at Site #4, when this signal was between 35 and 178 times as strong as anticipated for the assumed implant conditions.

For tests with a simulated ECG signal applied to the pacemaker, all pacemakers reverted to the asynchronous mode at some level of the interference waveform from all sites, with the exception of site #7. Site #7 was beneath the dc line which runs between Celilo and Sylmar. The signal recorded at this site could be raised to a factor of 178 above the reference level without causing reversion of any of the tested pacemakers, or without causing any observable rate deviation.

The pacemaker reversion test results are presented in Table 7.1. The data shown in this table were all obtained under the condition of a simulated ECG signal applied to the pacemaker under test. The table displays, for each pacemaker and test site, the factor by which the interference signal was adjusted from the reference condition to cause the onset of reversion. The onset of reversion is identified as when the pacemaker first starts to pulse. In general,

Table 7-1

MULTIPLYING FACTOR FOR ANTICIPATED PACEMAKER PICKUP
TO CAUSE ONSET OF REVERSION

	Measurement Site						
Pacemaker	1	2	3	4	5	6	7
1	0.7	3.2	1.6	35.5	0.32	11.2	> 178
2	0.7	3.2	1.6	35.5	0.28	11.2	"
3	0.2	1.6	0.9	20.0	0.14	5.6	"
4	1.0	4.0	2.0	35.5	0.5	15.8	"
5	1.1	4.5	2.2	35.5	0.56	20.0	"
6	0.6	1.8	1.0	15.8	0.13	7.0	"

NOTE: At sites 1, 2, 3, and 6, the 60 Hz signal was large relative to the harmonic components, as can be seen in the oscillographs shown in Appendix A. It was brought to our attention by one of the reviewers of this report that the empirically derived scale-u0 factors presented for sites 2 and 6 are larger than what would be calculated if the 60 Hz electric field component were the only one present. For example, using the known 60 Hz interference threshold of pacemaker #1 and the 60 Hz electric field component at site #6, a scale-up factor of about 3.5 would be expected. Paradoxically, the pacemakers have a higher threshold of interference for the more complicated waveform (i.e., including all of the harmonics and the magnetic field as well) than anticipated for the pure 60 Hz electric field waveform. However, no explanation for this effect is available at this time.

from 1 to 4 dB more signal than this was required to cause the pacemaker to fully revert, viz., to emit a steady train of pulses at the design reversion rate.

An example will serve to illustrate the table contents. Consider a specific pacemaker and site, i.e., a specific row and column in Table 7.1. The implicit conditions are that this pacemaker is implanted in a 50-percentile man. The pacemaker is in a monopolar abdominal location having a 15 cm electrode separation and a 210 cm^2 effective electrode loop. The patient is standing well grounded at the chosen site. Under these conditions, it is estimated that the pacemaker would evidence reversion onset if the fields at this site were adjusted by the factor shown in the table. As examples, consider pacemaker 1 and Site #1. the table shows that it is expected that the patient's pacemaker would revert if the fields at Site #1 were 0.7 times the levels which were measured.

The following paragraphs draw some general conclusions from the data presented in Table 7.1. Sites 1, 2 and 3 were beneath ac lines within the Celilo converter station. Figures A.1, A.2, and A.3 show that the electric fields at these three sites are virtually identical; however, the magnetic field spectra differ. Thus, the differences seen in columns 1-3 of Table 7.1 are apparently due to how the existing magnetic field induced components add to those due to the electric field. Site #1 was prior to any ac side filtering; the pacemakers were most sensitive to the composite waveform from this site. The fields measured at this site would cause reversion to most of the pacemakers.

The pacemakers were somewhat more sensitive to the fields under the line (Site #3) leading to the ac side filter group than they were to the fields from the ac line after filtering (Site #2). Since the 5th and 7th harmonics are filtered at Big Eddy rather than at Celilo, 5th and 7th harmonic current flow in the line at Site #2, but at a reduced level at Site #3. Thus, the added sensitivity at Site #3 is possibly due to the higher frequency harmonic components of current which flows in the line at Site #3. The fields at Sites #2 and #3 are, in general, less than required for pacemaker reversion.

Comparison of the tabulated data for Sites #4 and #5 show the effect of the dc filter group in reducing interference-producing field components. Site #4 (after the filters) is considerably less interference prone than is Site #5 (before the filters). The fields at site #5 should be anticipated to cause reversion of all of the pacemakers tested, for the assumed implant conditions. However, at site #4, no pacemaker reversion is anticipated, with a rather large safety margin.

The reversion data shown for Site #6 reflects the effect of the greater transmission line height at that site. None of the pacemakers should revert at this site.

The data of Table 7.1 for Site #7 is considered significant. The data shows that the fields at this site are considerably less than necessary for pacemaker reversion. No reversion in the bench tests was caused when the effective magnitude of these fields was increased by over 100 times the levels measured at the site. If the fields measured at this site are indicative of those existing along the length of the Pacific Intertie, then it appears that a significant safety margin exists with respect to potential interference to implanted pacemakers.

Section 8

REFERENCES

1. J.E. Bridges and M.J. Frazier, "The Effects of 60 Hz Electric and Magnetic Fields on Patients with Implanted Cardiac Pacemakers". IIT Research Institute Project No. E8167 Final Report, EPRI Contract No. RP679-1 (in press).

2. D.A. Miller, "Susceptibility of Cardiac Pacemakers to ELF Magnetic Fields". Technical Memorandum No. 1, IITRI Project E6185, U.S. Naval Electronic Systems Command Contract No. N00039-71-C-0111 (April 1971).

3. T.D. Bracken, "Field Measurements and Calculations of Electrostatic Effects of Overhead Transmission Lines", IEEE Paper F75-573-6, presented at 1975 IEEE Power Meeting, San Francisco, California.

4. D.W. Deno, "Currents Induced in the Human Body by High Voltage Transmission Line Electric Field Measurement and Calculation of Distributed Dose". IEEE Transactions on Power Apparatus and Systems, Vol. PAS-96, No. 5, September/October 1977.

5. H. Dreyfuss. The Measure of Man. (New York: Whitney Publications, 1959).

6. R. Gamboa and B.N. Adair, "Thorax Resistivity in Children and Adults". Journal of Applied Physics, 23 (1967), pp. 109-113.

APPENDIX A

PHOTOGRAPHS OF $\dot{E}$ AND $\dot{B}$ SENSOR OUTPUTS (TIME AND SPECTRAL) FOR THE SEVEN CELILO MEASUREMENT SITES

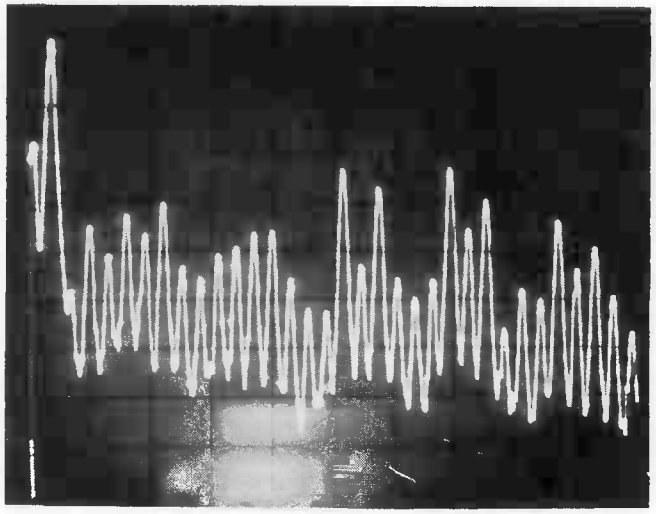

$\dot{E}$ Sensor Spectrum, -10 dB Full Scale
200 Hz per division

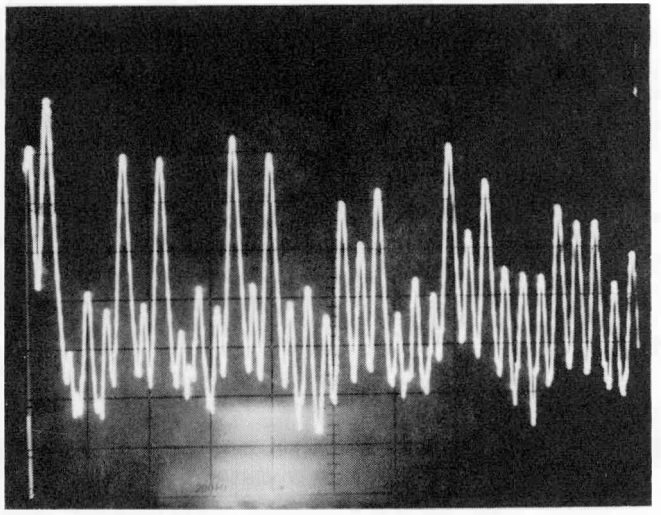

$\dot{B}$ Sensor Spectrum, -20 dBV Full Scale
200 Hz per division

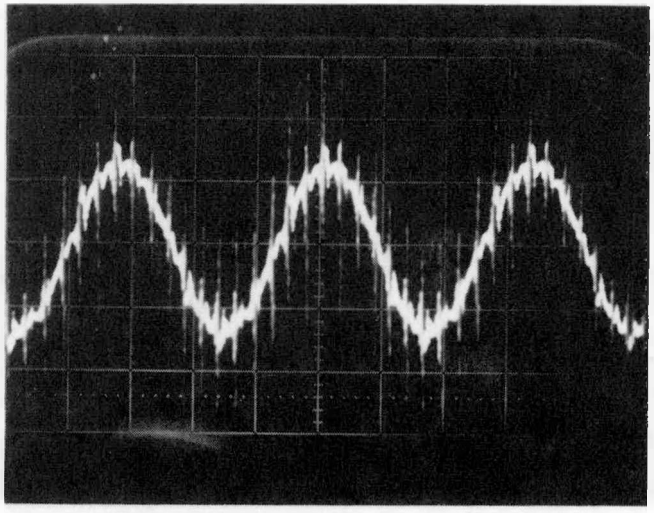

$\dot{E}$ Sensor Time Waveform
0.2 V/div., 5 ms/div.

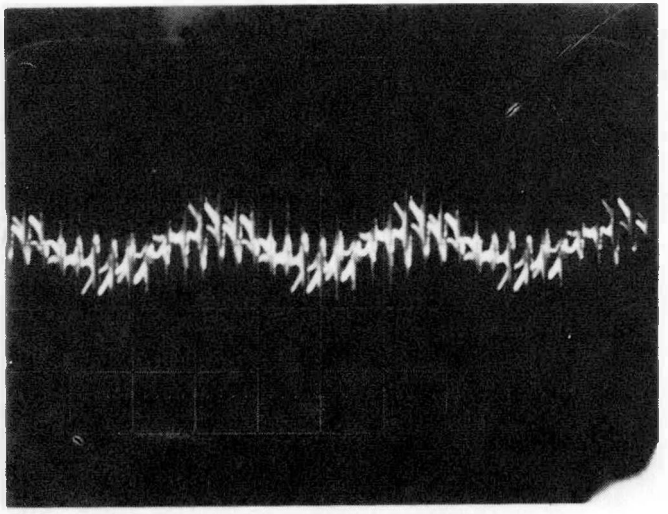

$\dot{B}$ Sensor Time Waveform
0.1 V/div., 5 ms/div.

Figure A.1 $\dot{E}$ AND $\dot{B}$ SPECTRUM AND WAVEFORMS AT SITE 1

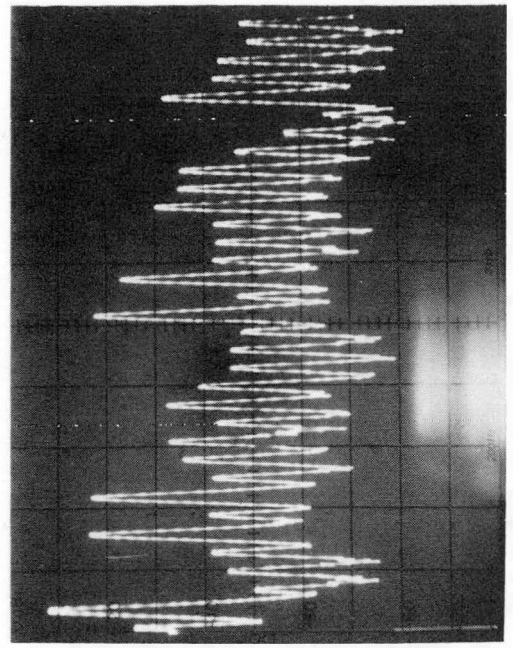

$\dot{B}$ Sensor Spectrum, -20 dBV Full Scale
200 Hz per division

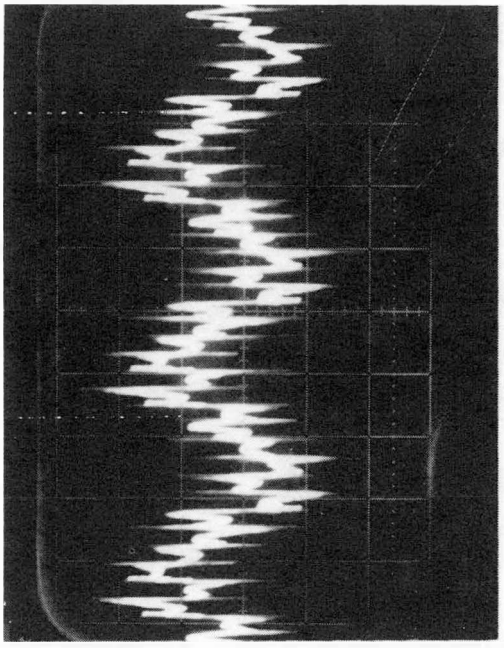

$\dot{B}$ Sensor Time Waveform
0.1 V/div., 5 ms/div.

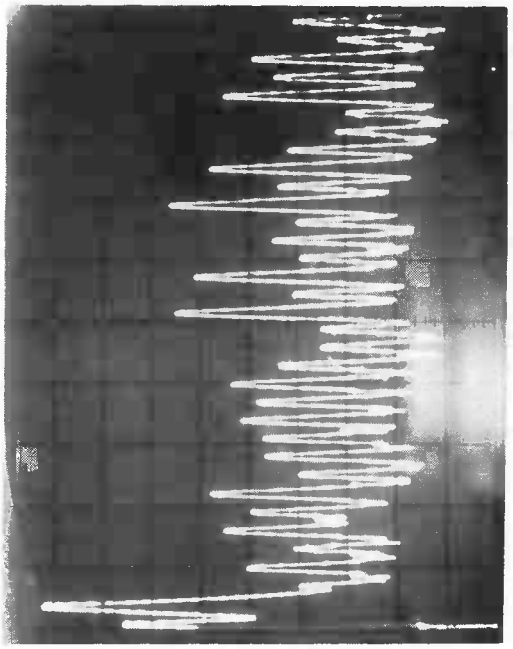

$\dot{E}$ Sensor Spectrum, -10 dB Full Scale
200 Hz per division

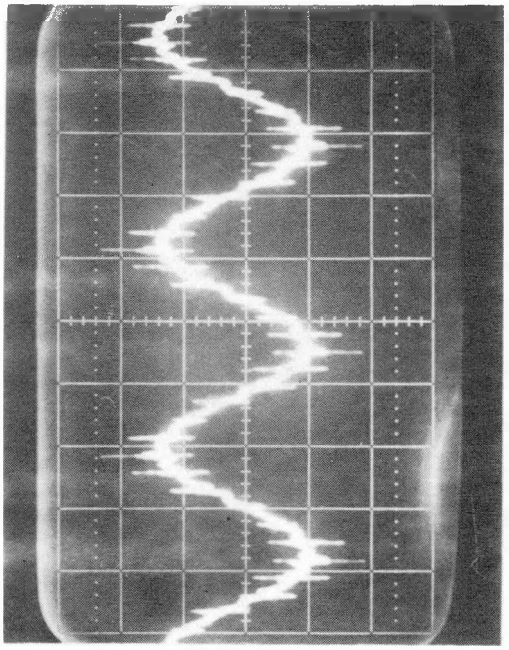

$\dot{E}$ Sensor Time Waveform
0.2 V/div., 5 ms/div.

Figure A.2 $\dot{E}$ AND $\dot{B}$ SPECTRUM AND WAVEFORMS AT SITE 2

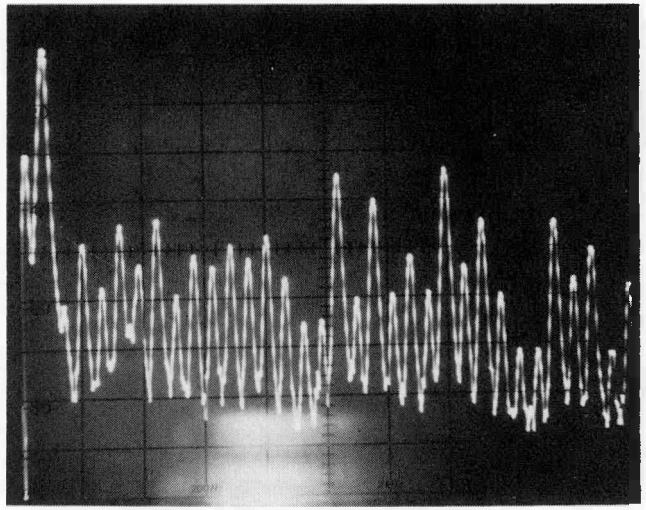

$\dot{E}$ Sensor Spectrum, -70 dBV Full Scale
200 Hz/div.

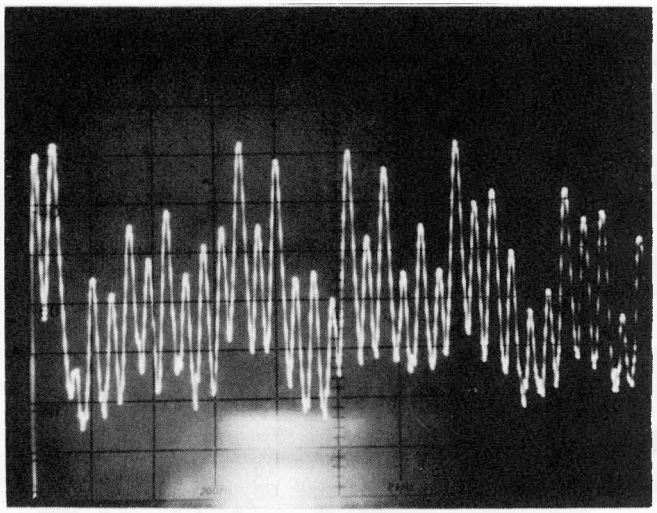

$\dot{B}$ Sensor Spectrum, -10 dBV Full Scale
200 Hz/div.

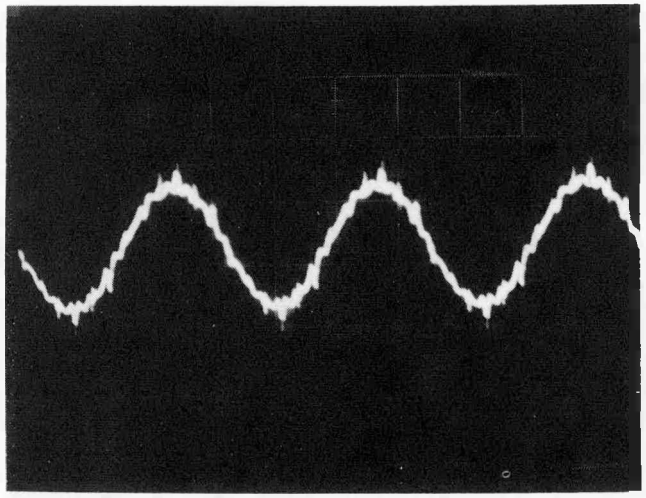

E Sensor Time Waveform, 0.20/div
5 ms/div.

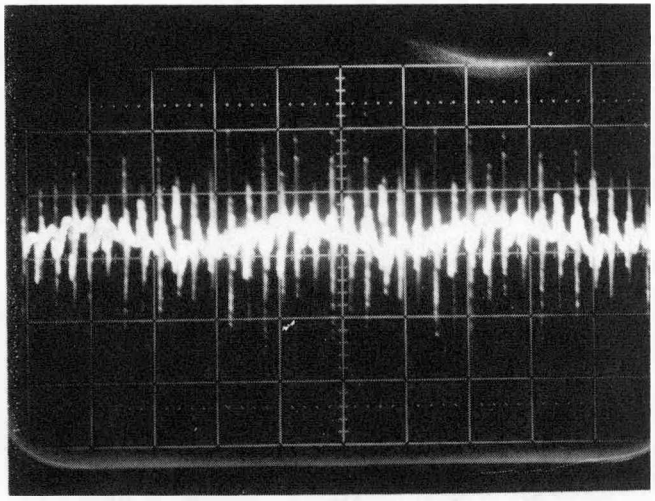

B Sensor Time Waveform, 0.2 V/div.
5 ms/div.

Figure A.3 $\dot{E}$ AND $\dot{B}$ SPECTRUM AND WAVEFORMS AT SITE 3

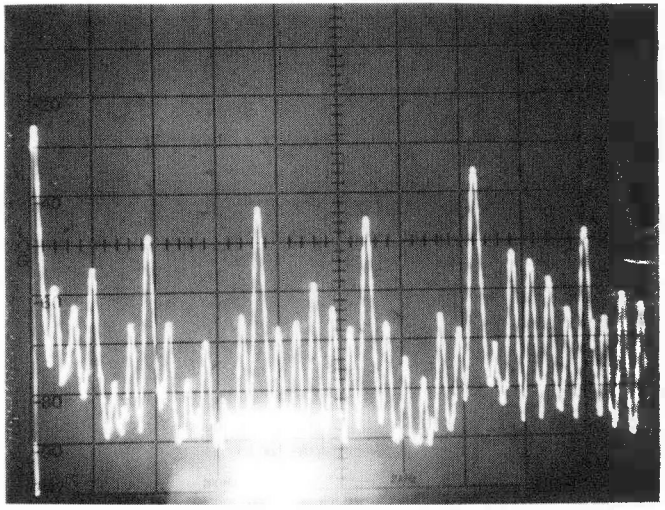

$\dot{E}$ Sensor Spectrum, -10 dBV Full Scale
200 Hz/div.

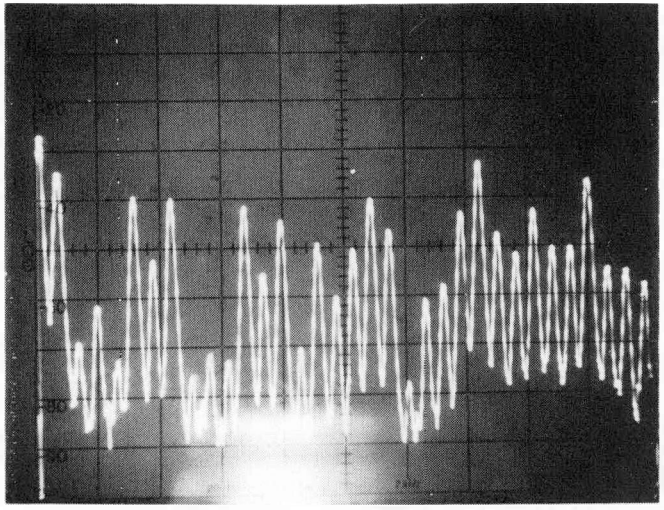

$\dot{B}$ Sensor Spectrum, -20 dBV Full Scale
200 Hz/ div.

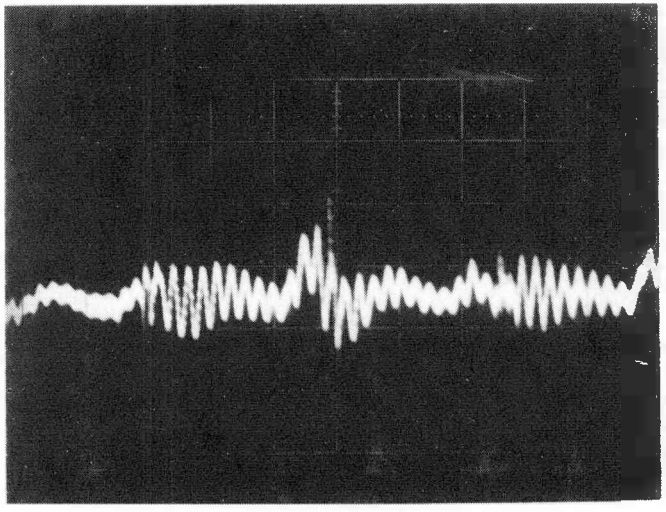

$\dot{E}$ Sensor Time Waveform
0.05 V/div., 500 μs/div.

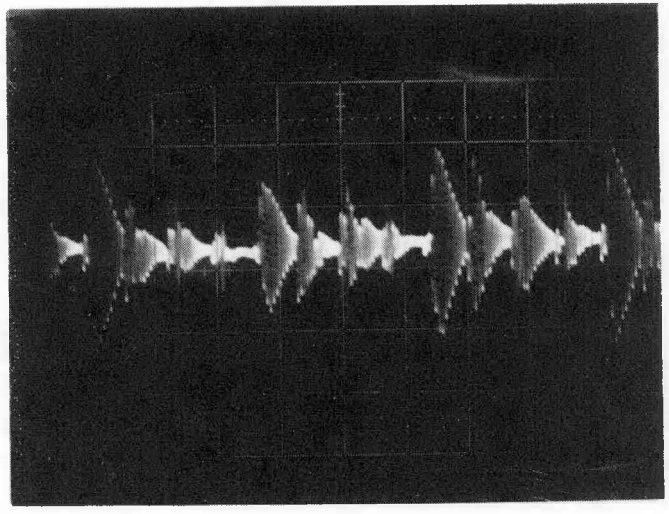

$\dot{B}$ Sensor Time Waveform
0.1 V/div., 2 ms/div.

Figure A.4 $\dot{E}$ AND $\dot{B}$ SPECTRUM AND WAVESHAPE AT SITE 4

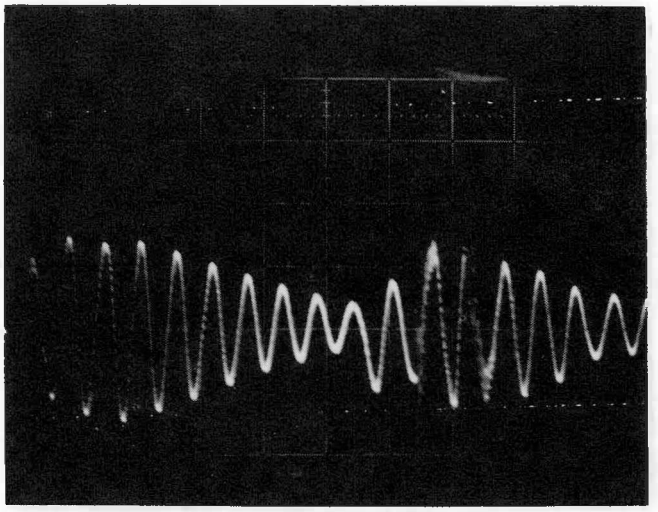

200 μs/div.
0.1 V/div.

Figure A.5 B WAVEFORM AT SITE 4

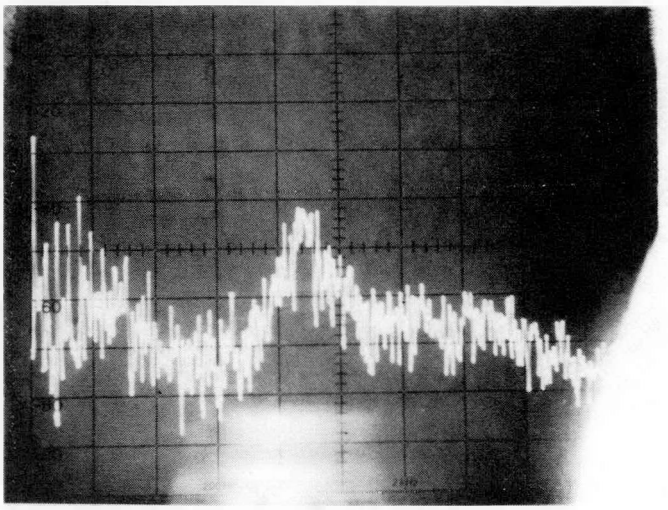

-10 dBV Full Scale
2 kHz/div.

Figure A.6 WIDEBAND B SPECTRUM AT SITE 4

The measurements at site 5 are affected by the valve commutations. Site 4 must have been shielded from the wall bushings of group 6, since the commutations do not show up with any significant amplitude.

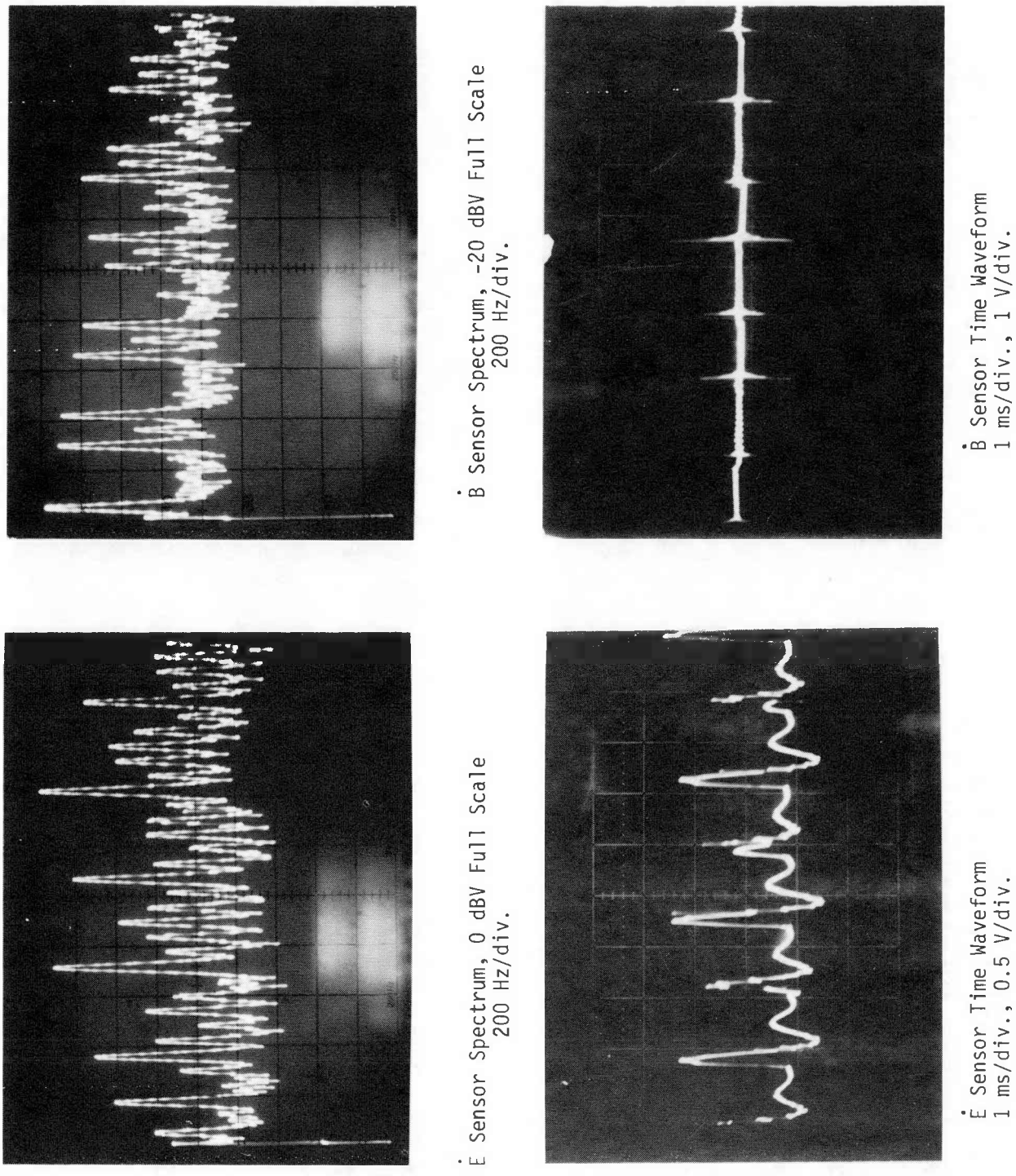

Figure A.7 $\dot{E}$ AND $\dot{B}$ SPECTRA AND WAVESHAPES AT SITE 5

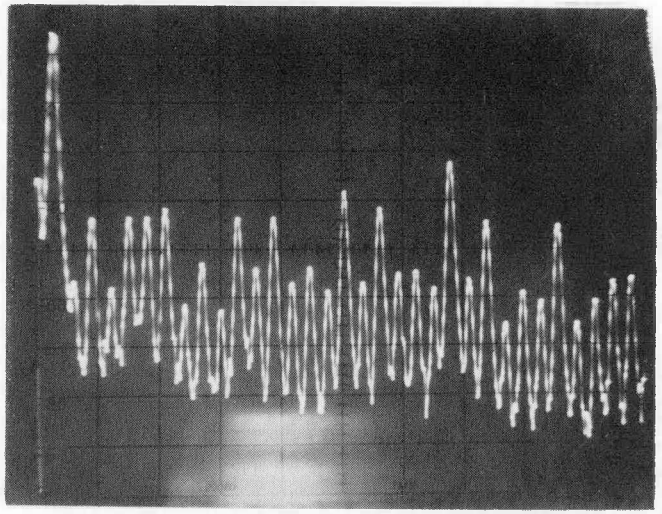

$\dot{E}$ Spectrum, -20 dBV Full Scale
200 Hz/div.

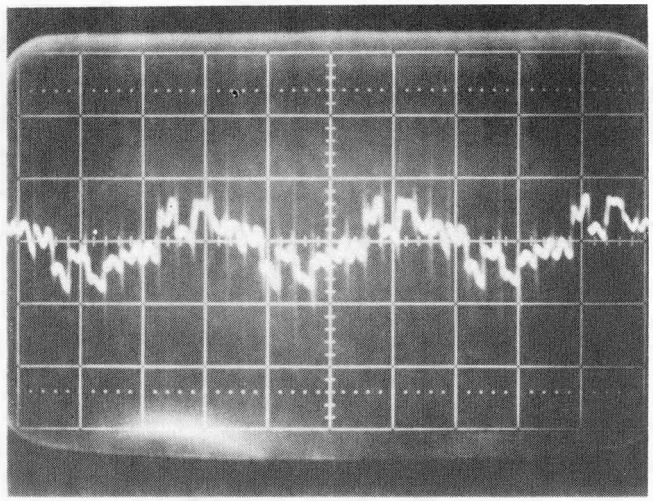

$\dot{B}$ Sensor Time Waveform
0.05 V/div, 5 ms/div.

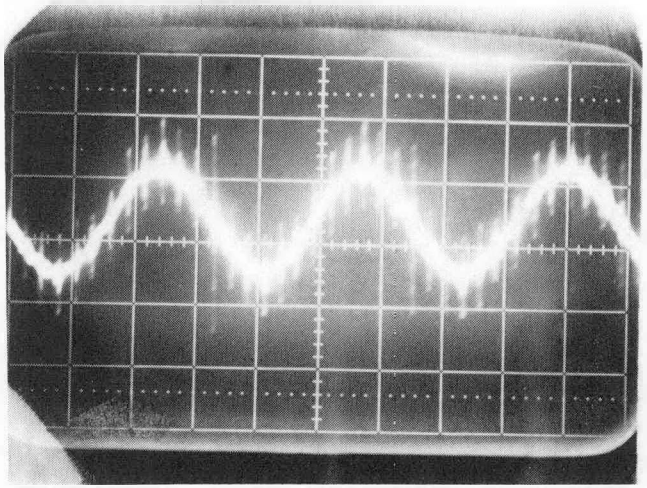

$\dot{E}$ Sensor Time Waveform
0.2 V/div., 5 ms/div.

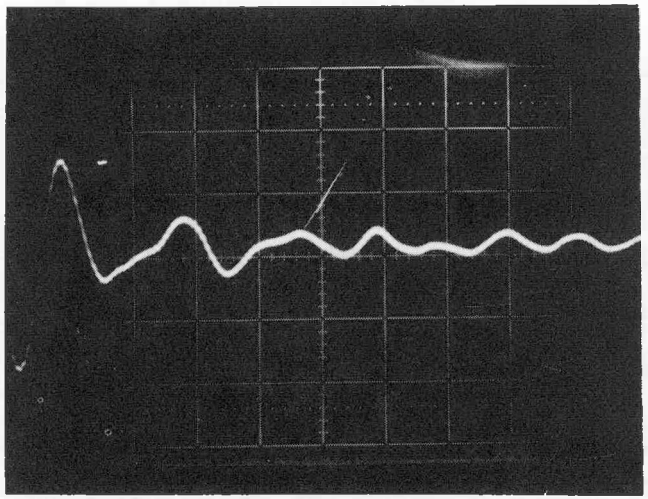

$\dot{E}$ Sensor Ringing Waveform
10 μs/div., 0.1 V/div.

Figure A.8 $\dot{E}$ AND $\dot{B}$ SPECTRA AND WAVESHAPES AT SITE 6

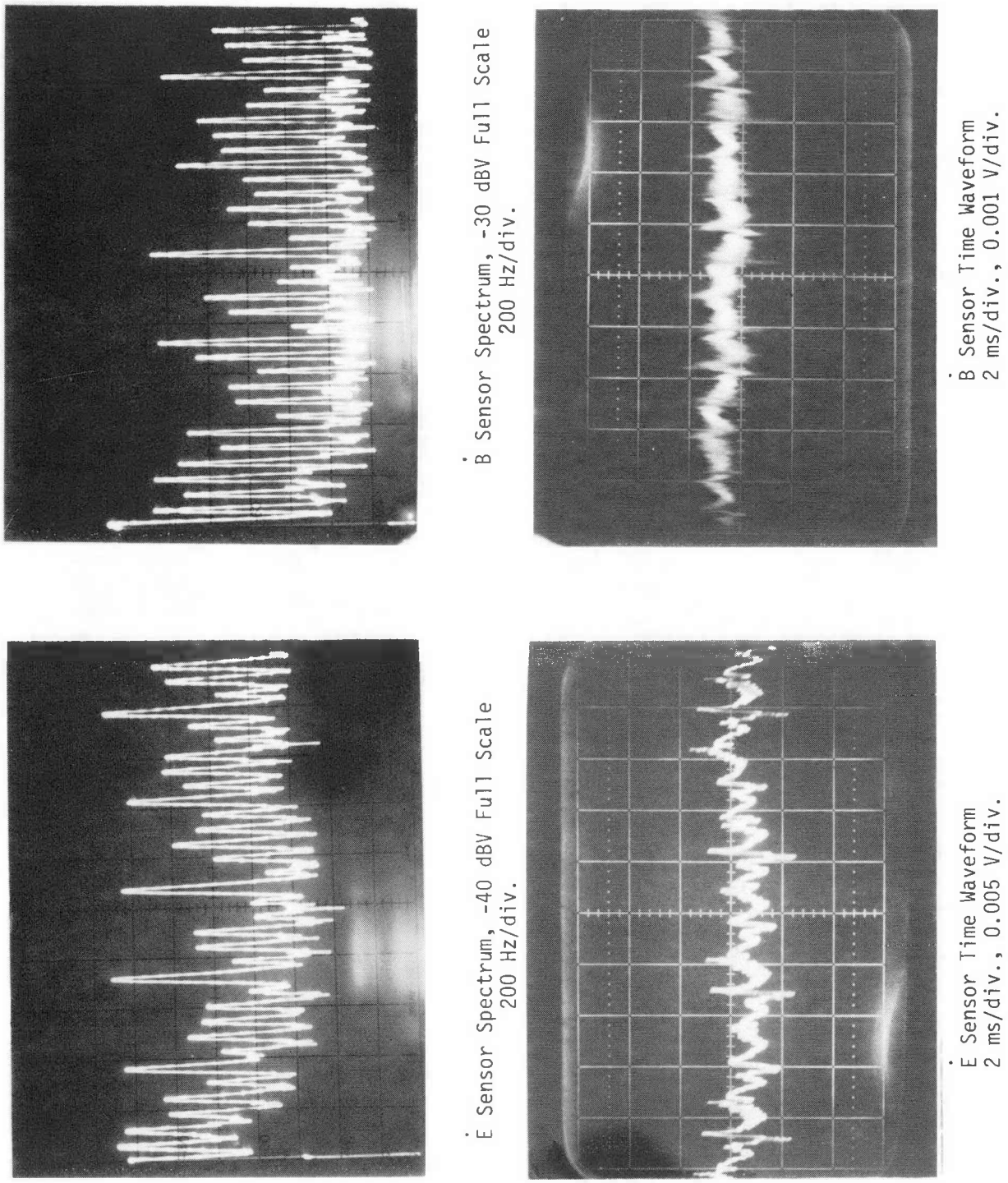

Figure A.9 $\dot{E}$ AND $\dot{B}$ SPECTRA AND WAVESHAPES AT SITE 7